Frequency metrology of buffer-gas-cooled molecular spectra for fundamental Physics research

Pasquale Maddaloni
Cold Molecules lab @ INO Pozzuoli

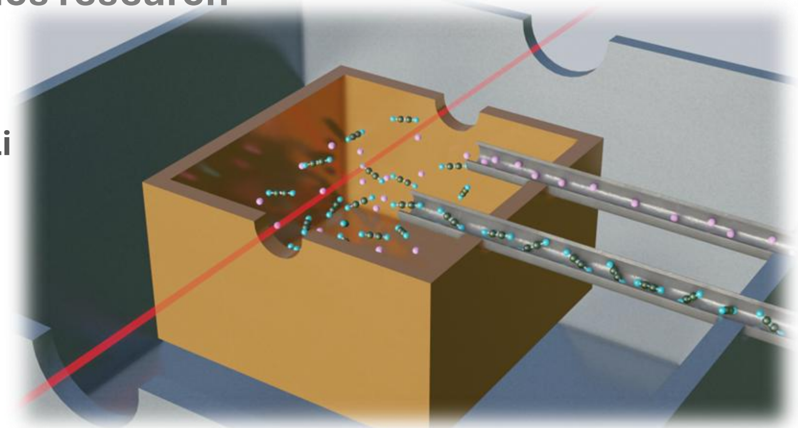

The Low-Energy Frontier of Particle Physics
INFN-LNF, 10-12 feb 2025

The flaws of the Standard Model (SM)

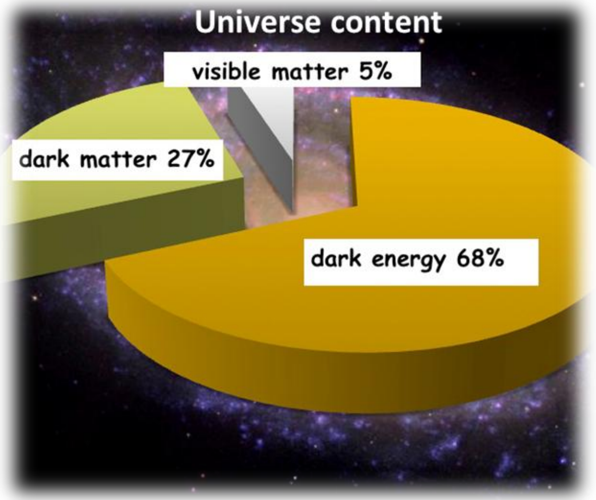

While currently a bedrock in our understanding of fundamental physical interactions, the SM fails to explain cosmological observations of the energy and matter content in the Universe

• **Neutrino oscillations**. In the SM, neutrinos are massless particles since they do not couple to the Higgs. However, it is an empirical fact that neutrinos change flavor as they travel long distances, implying a small mass.

• **The strong CP problem**. Quantum chromodynamics preserves the charge conjugation-parity symmetry although, a priori, there is no reason for it. This problem can be solved by invoking the existence of a new particle (Peccei and Quinn hypothesis): the axion, which is not included in the SM.

• **Dark Matter (DM)**. From the rotation curves of galaxies to the large-structure of the universe, there are strong evidences of the existence of DM. Despite its ubiquitousness, its nature remains a mystery due to the large mass range in which one may expect signals from SM-DM particles interactions.

• **Dark energy**. It is a global energy that accelerates the expansion of the universe, although its nature is unknown.

• **Baryogenesis.** The SM predicts that matter and antimatter should be created equally in almost any process. However, the baryonic matter of the universe (i.e., excluding DM) appears to be constituted of fundamental particles instead of anti-particles.

Low-energy New Physics (NP) probes

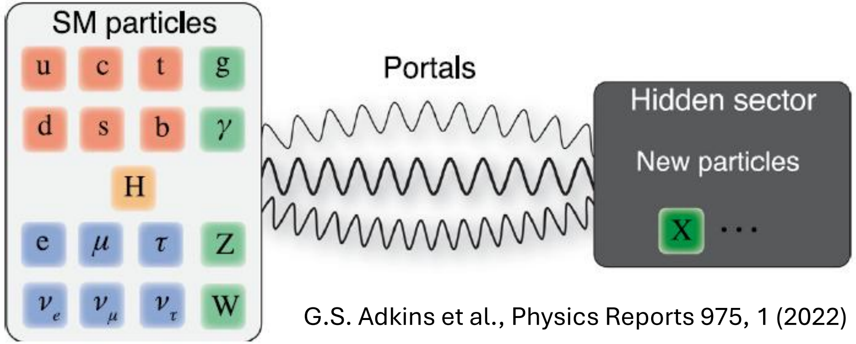

G.S. Adkins et al., Physics Reports 975, 1 (2022)

Among the theoretical models that accommodate some of the phenomenology that the SM cannot explain one well-motivated framework is the **hidden sector**, assuming that a set of fields and symmetries are hidden in nature. **The hidden and visible sectors interact through portals containing mediators between new particles and the SM model ones** (e.g., the dark photon in the case of dark matter).

Low-energy New Physics (NP) probes

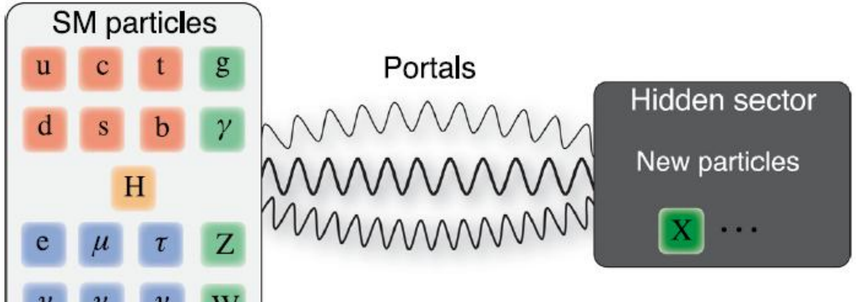

G.S. Adkins et al., Physics Reports 975, 1 (2022)

Among the theoretical models that accommodate some of the phenomenology that the SM cannot explain one well-motivated framework is the **hidden sector**, assuming that a set of fields and symmetries are hidden in nature. **The hidden and visible sectors interact through portals containing mediators between new particles and the SM model ones** (e.g., the dark photon in the case of dark matter).

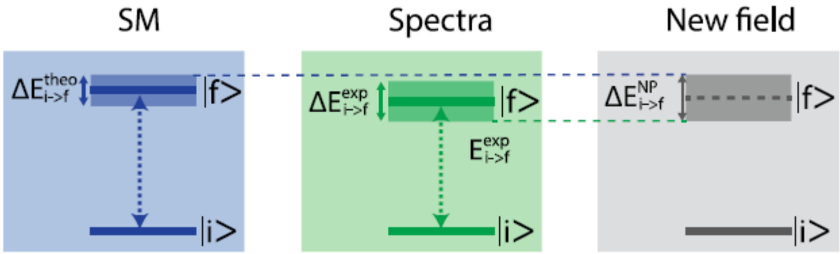

NP ⇒ new Hamiltonian terms ⇒ shifts in atomic/molecular spectra

“Most physicists asked to think of searches for Physics beyond the SM immediately picture multi-billion-dollar particle accelerators with detectors the size of office buildings, as very high energies (TeV) are required to produce and detect exotic particles. In fact, though, modern **laser spectroscopy** *of atoms and molecules allows measurements of astonishing precision, sufficient to detect the subtle influence of new fundamental Physics at the eV energy scale.”* C. Orzel, Phys. Scr. 86, 068101 (2012)

Current AMO-based searches

REVIEWS OF MODERN PHYSICS, VOLUME 90, APRIL–JUNE 2018

Search for new physics with atoms and molecules

M. S. Safronova

University of Delaware, Newark, Delaware 19716, USA
and Joint Quantum Institute, National Institute of Standards and Technology
and the University of Maryland, College Park, Maryland 20742, USA

D. Budker

Helmholtz Institute, Johannes Gutenberg University, Mainz, Germany,
University of California, Berkeley, California 94720, USA,
and Nuclear Science Division, Lawrence Berkeley National Laboratory,
Berkeley, California 94720, USA

D. DeMille

Yale University, New Haven, Connecticut 06520, USA

Derek F. Jackson Kimball

California State University, East Bay, Hayward, California 94542, USA

A. Derevianko

University of Nevada, Reno, Nevada 89557, USA

Charles W. Clark

Joint Quantum Institute, National Institute of Standards and Technology
and the University of Maryland, College Park, Maryland 20742, USA

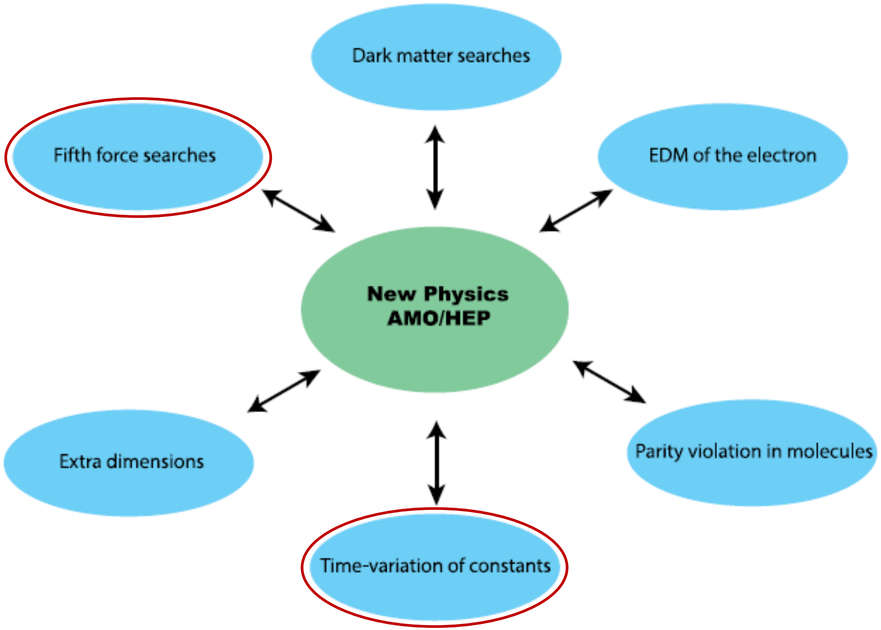

The additional degrees of freedom available in **molecules** (vibrations, rotations, Λ-doubling, Fermi resonances,...), while presenting complexities and challenges for experimental control, provide a richer (compared to atoms) playground for precision measurements and higher sensitivity to certain phenomena

Current AMO-based searches

REVIEWS OF MODERN PHYSICS, VOLUME 90, APRIL–JUNE 2018

Search for new physics with atoms and molecules

M. S. Safronova

University of Delaware, Newark, Delaware 19716, USA
and Joint Quantum Institute, National Institute of Standards and Technology
and the University of Maryland, College Park, Maryland 20742, USA

D. Budker

Helmholtz Institute, Johannes Gutenberg University, Mainz, Germany,
University of California, Berkeley, California 94720, USA,
and Nuclear Science Division, Lawrence Berkeley National Laboratory,
Berkeley, California 94720, USA

D. DeMille

Yale University, New Haven, Connecticut 06520, USA

Derek F. Jackson Kimball

California State University, East Bay, Hayward, California 94542, USA

A. Derevianko

University of Nevada, Reno, Nevada 89557, USA

Charles W. Clark

Joint Quantum Institute, National Institute of Standards and Technology
and the University of Maryland, College Park, Maryland 20742, USA

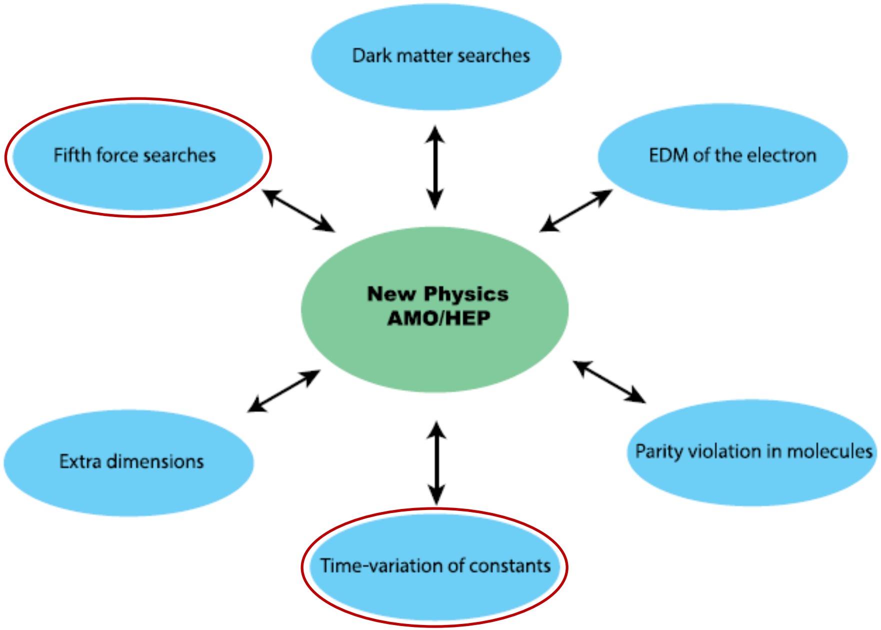

The additional degrees of freedom available in **molecules** (vibrations, rotations, Λ-doubling, Fermi resonances,...), while presenting complexities and challenges for experimental control, provide a richer (compared to atoms) playground for precision measurements and higher sensitivity to certain phenomena

Ultra-accurate **frequency measurements** of **ro-vibrational** transitions in **neutral stable** molecules

Absolute frequency metrology of cold ro-vibrational spectra

1. Infrared narrow-linewidth and highly stable laser sources with absolute frequency calibration

✓ prestabilization against ultra-stable cavities, referencing to atomic clocks via optical frequency comb synthesizers, metrological optical fiber links,...

Absolute frequency metrology of cold ro-vibrational spectra

1. Infrared narrow-linewidth and highly stable laser sources with absolute frequency calibration

✓ prestabilization against ultra-stable cavities, referencing to atomic clocks via optical frequency comb synthesizers, metrological optical fiber links,...

2. High-resolution and high-sensitivity (cavity-enhanced) spectroscopic techniques

✓ Lamb-dip spectroscopy, two-photon spectroscopy, Ramsey fringes,...

$$\delta\nu_0 \sim \frac{\Gamma}{SNR} = \frac{\Gamma_{nat} + \Gamma_{laser} + \Gamma_{coll} + \Gamma_{transit} + \ldots}{SNR} \simeq$$

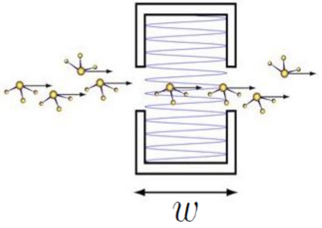

$$\simeq \frac{\Gamma_{transit}}{SNR} \propto \frac{1}{w}\sqrt{\frac{k_B T}{m}}\frac{1}{SNR}$$

Absolute frequency metrology of cold ro-vibrational spectra

1. Infrared narrow-linewidth and highly stable laser sources with absolute frequency calibration

✓ prestabilization against ultra-stable cavities, referencing to atomic clocks via optical frequency comb synthesizers, metrological optical fiber links,…

2. High-resolution and high-sensitivity (cavity-enhanced) spectroscopic techniques

✓ Lamb-dip spectroscopy, two-photon spectroscopy, Ramsey fringes,…

$$\delta\nu_0 \sim \frac{\Gamma}{SNR} = \frac{\Gamma_{nat} + \Gamma_{laser} + \Gamma_{coll} + \Gamma_{transit} + \ldots}{SNR} \simeq$$

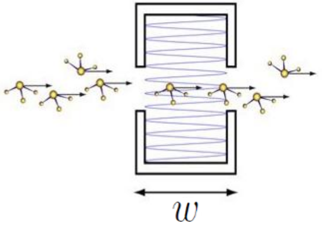

$$\simeq \frac{\Gamma_{transit}}{SNR} \propto \frac{1}{w}\sqrt{\frac{k_B T}{m}}\frac{1}{SNR}$$

3. Samples of cold (slow) stable molecules (hydrides, nitrides, oxides, fluorides,…) to enhance the spectroscopic interrogation time

PROCEEDINGS A

Review

Check for updates

Cite this article: Softley TP. 2023 Cold and ultracold molecules in the twenties. *Proc. R. Soc. A* **479**: 20220806.

Cold and ultracold molecules in the twenties

Timothy P. Softley

School of Chemistry, University of Birmingham, Edgbaston, Birmingham B15 2TT, UK

L. Santamaria et al., Int. J. Mol. Sci. 22, 250 (2021) P. Maddaloni et al., Rivista del Nuovo Cimento 40, 135 (2017)

Cold Molecules for Quantum Science and Technology

Photo/Magneto-association of ultracold atoms

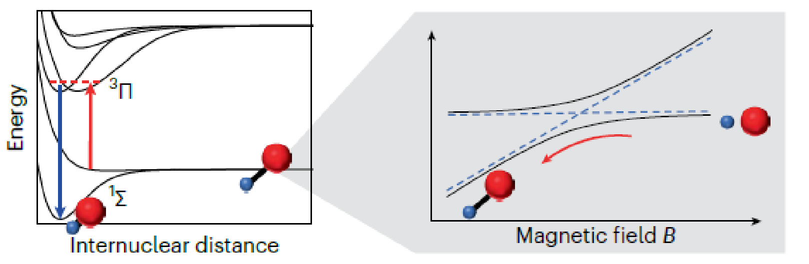

Pairs of atoms are associated into a weakly bound molecule by sweeping a magnetic field over a scattering (Feshbach) resonance. These weakly bound molecules (dimers) are subsequently transferred into the rovibrational ground state by a STIRAP via an excited state.

Cold Molecules for Quantum Science and Technology

Photo/Magneto-association of ultracold atoms

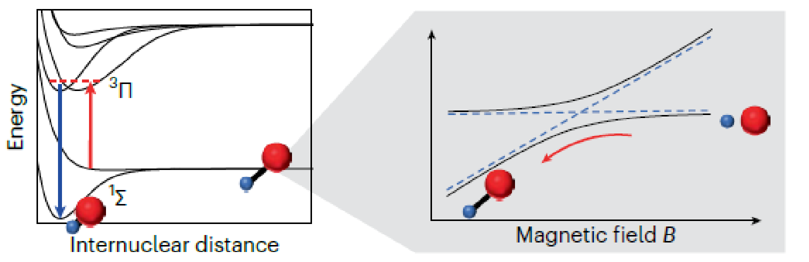

Pairs of atoms are associated into a weakly bound molecule by sweeping a magnetic field over a scattering (Feshbach) resonance. These weakly bound molecules (dimers) are subsequently transferred into the rovibrational ground state by a STIRAP via an excited state.

Direct cooling of ground-state molecules

Cold Molecules for Quantum Science and Technology

Photo/Magneto-association of ultracold atoms

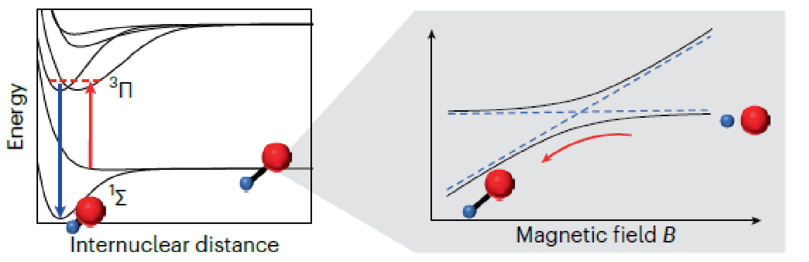

Pairs of atoms are associated into a weakly bound molecule by sweeping a magnetic field over a scattering (Feshbach) resonance. These weakly bound molecules (dimers) are subsequently transferred into the rovibrational ground state by a STIRAP via an excited state.

Direct cooling of ground-state molecules

nature physics

Review article https://doi.org/10.1038/s41567-024-02453-9

Quantum computation and quantum simulation with ultracold molecules

Received: 5 August 2023

Accepted: 26 February 2024

Simon L. Cornish[1], Michael R. Tarbutt[2] & Kaden R. A. Hazzard[3]

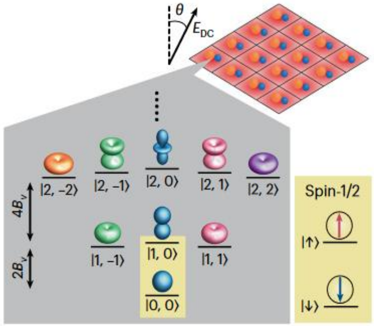

Pseudo-spins (or qubits) can be encoded in the rotational states of ultracold polar molecules confined in optical lattices (or tweezer arrays) for applications in quantum simulation (condensed-matter phenomena) and computation.

Cold Molecules for Quantum Science and Technology

Photo/Magneto-association of ultracold atoms

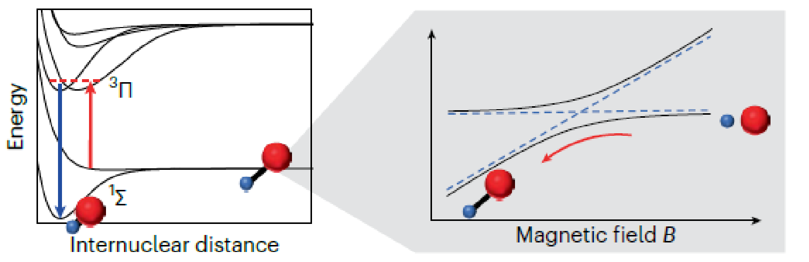

Pairs of atoms are associated into a weakly bound molecule by sweeping a magnetic field over a scattering (Feshbach) resonance. These weakly bound molecules (dimers) are subsequently transferred into the rovibrational ground state by a STIRAP via an excited state.

Direct cooling of ground-state molecules

nature physics

Review article https://doi.org/10.1038/s41567-024-02453-9

Quantum computation and quantum simulation with ultracold molecules

Received: 5 August 2023

Accepted: 26 February 2024

Simon L. Cornish [1], Michael R. Tarbutt [2] & Kaden R. A. Hazzard [3]

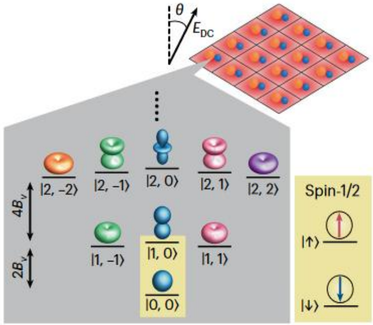

Pseudo-spins (or qubits) can be encoded in the rotational states of ultracold polar molecules confined in optical lattices (or tweezer arrays) for applications in quantum simulation (condensed-matter phenomena) and computation.

nature physics

Review article https://doi.org/10.1038/s41567-024-02499-9

Quantum sensing and metrology for fundamental physics with molecules

Received: 10 August 2023

Accepted: 2 April 2024

David DeMille [1,2], Nicholas R. Hutzler [3], Ana Maria Rey [4,5] & Tanya Zelevinsky [6]

⇒ Towards fully quantum metrology: entanglement in an array of quantum systems, enabling uncertainty reduction below the standard quantum limit

Buffer Gas Cooling

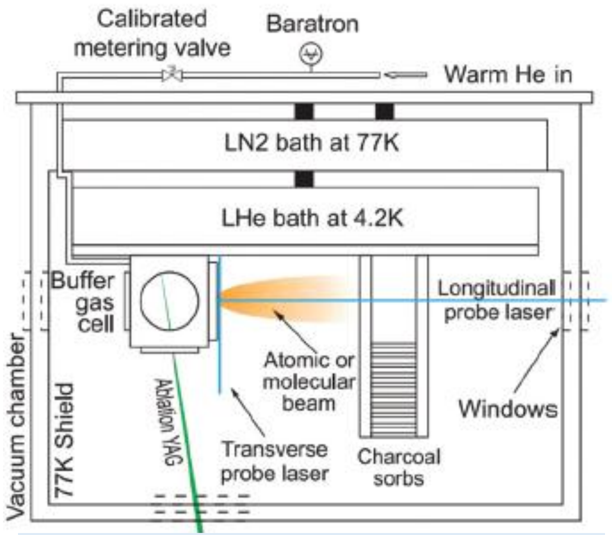

The molecular species is cooled via collisions with a thermal bath of helium in a copper cell in thermal contact with the cold plate (4 K) of a cryostat; then, a molecular beam is formed by expansion in a high vacuum (partially-hydrodynamic regime).

J.K. Messer et al., Phys. Rev. Lett. 53, 2555 (1984)
S.E. Maxwell et al., Phys. Rev. Lett. 95, 173201 (2005)

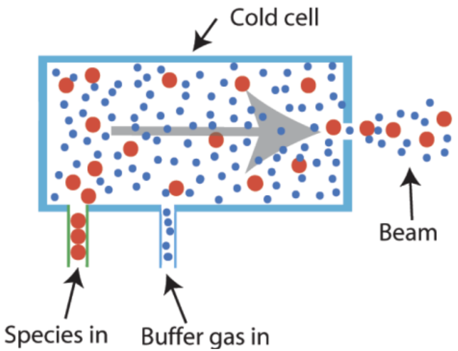

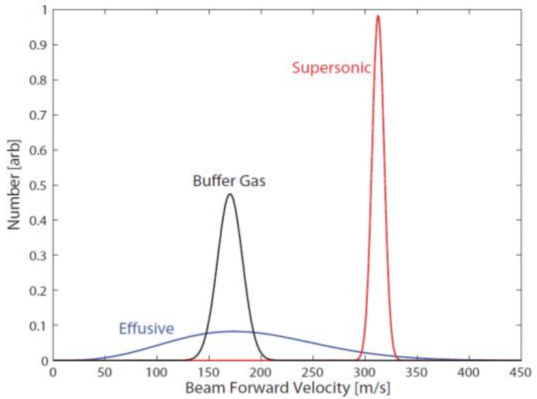

Reduced mean forward velocity (u) and temperature (i.e. spread around u)

Buffer Gas Cooling + Stark deceleration

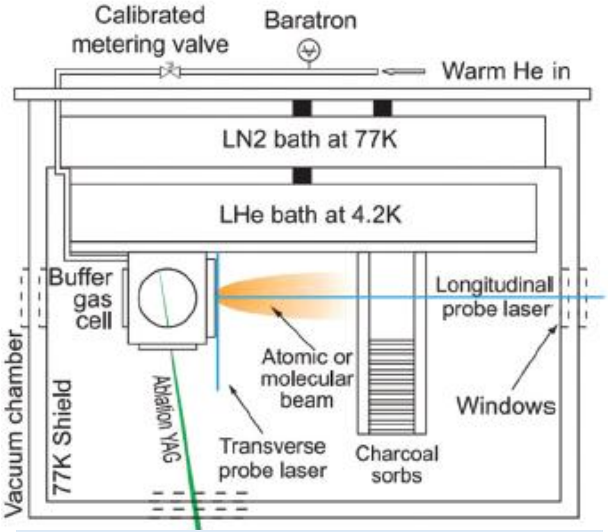

The molecular species is cooled via collisions with a thermal bath of helium in a copper cell in thermal contact with the cold plate (4 K) of a cryostat; then, a molecular beam is formed by expansion in a high vacuum (partially-hydrodynamic regime).

J.K. Messer et al., Phys. Rev. Lett. 53, 2555 (1984)
S.E. Maxwell et al., Phys. Rev. Lett. 95, 173201 (2005)

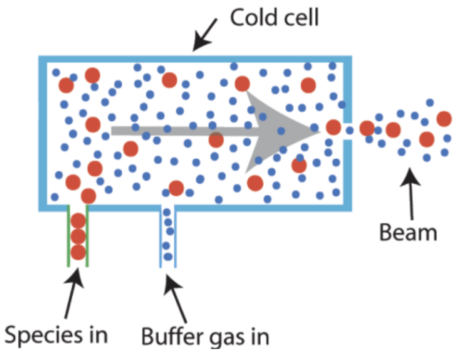

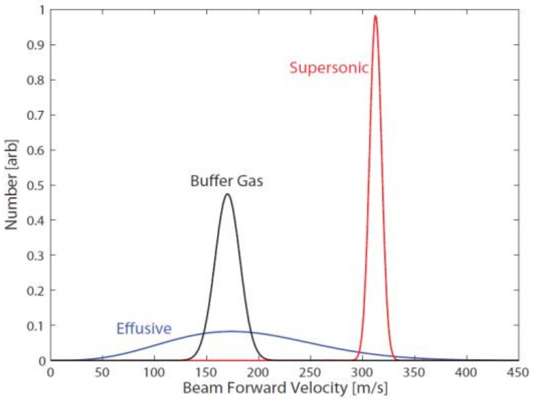

Reduced mean forward velocity (u) and temperature (i.e. spread around u)

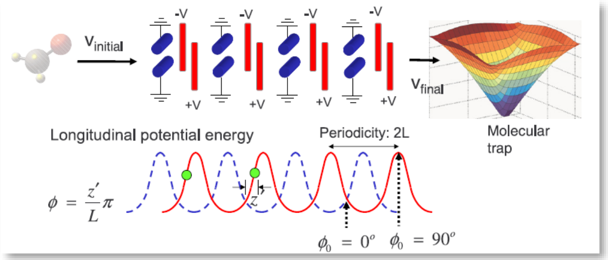

The molecular dipole moment interacts with a time-varying electric field gradient → loss of kinetic energy is due to the coerced gain of Stark potential (Sisyphus-type scheme)

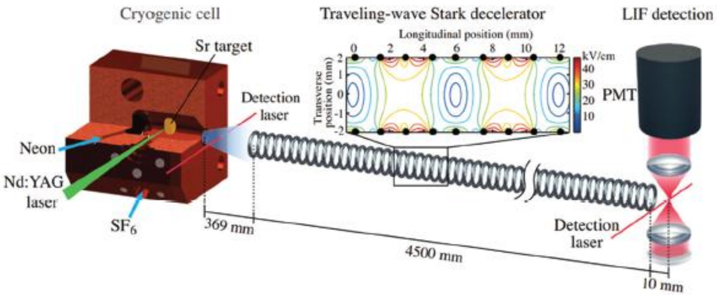

P. Aggarwal et al., Phys. Rev. Lett. 127, 173201 (2021)

Buffer Gas Cooling + Laser cooling

Laser cooling relies on the **repeated scattering of photons** (the collective actions of tens of thousands of photons, each with a small individual momentum, lead to sizable dissipative forces)

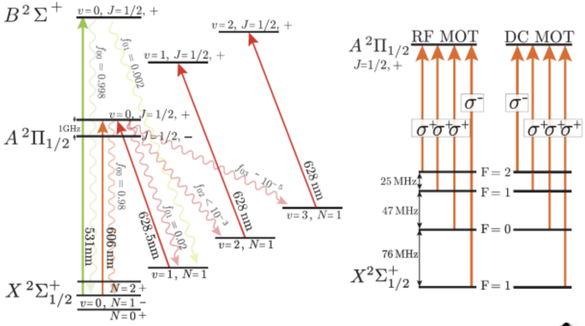

Several species have been shown to possess a highly **diagonal Franck-Condon matrix** and favorable transition selection rules to limit vibrational and rotational branching. For example, alkaline earth monofluorides (e.g. SrF, CaF) behave similarly to alkali atoms

The complex structure of molecules makes it difficult to find **a closed cycling transition** (an excitation created by absorbing a photon can easily decay into many vibrational and rotational energy levels different from the initial one)

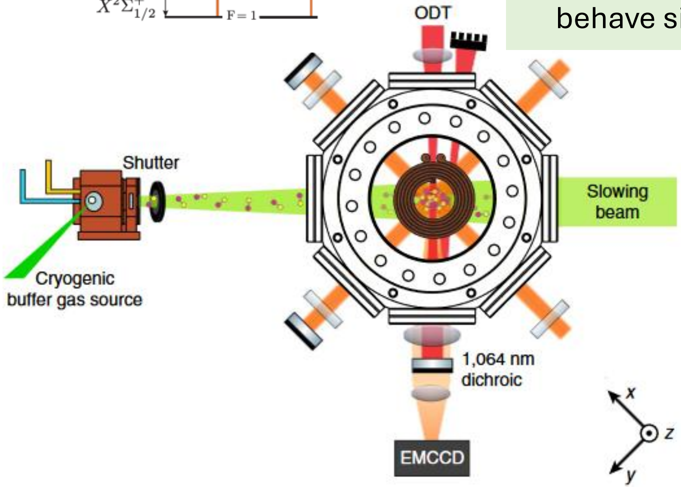

→ a few re-pumping lasers are enough to accompany the main cooling transition

Sub-Doppler cooling (MOT followed by molasses) + far-detuned optical dipole trap (ODT)

$$n \cong 8 \cdot 10^{7}\ cm^{-3},\ T \cong 60\ \mu K, \rho \cong 2 \cdot 10^{-9}$$

L. Anderegg et al., Nature Physics 119, 103201 (2018)
N.J. Fitch et al., AAMOP 70, 157 (2021)
B.L. Augenbraun et al., AAMOP 72, 89 (2023)
T.K. Langin et al., New J. Phys. 25, 043005 (2023)

➡ **Evaporative or Symphatetic cooling**

Precision ro-vibrational spectroscopy of Buffer-Gas-Cooled Molecules

- ✓ Any molecular species at rotational and translational temperatures of a few K
- ✓ Improves state selectivity → reduced spectral congestion, increased absorption cross-sections
- ✓ Restricts the distribution of velocities in the sample → narrower lineshapes
- ✓ Suppresses collisional broadening effects (when using specimens in form of beams)

Great potential for accurate line-center frequency measurements

Infrared cavity-enhanced direct frequency comb spectroscopy (CE-DFCS) of large species or complex chemical mixtures: vinyl bromide, diamantane, nitromethane, naphthalene, hexamethylenetetramine,…

Spaun et al., Nature 533, 517 (2016)
Changala et al., Science 363, 49 (2019)

Quantum state-resolved ro-vibrational transitions in C60 fullerene

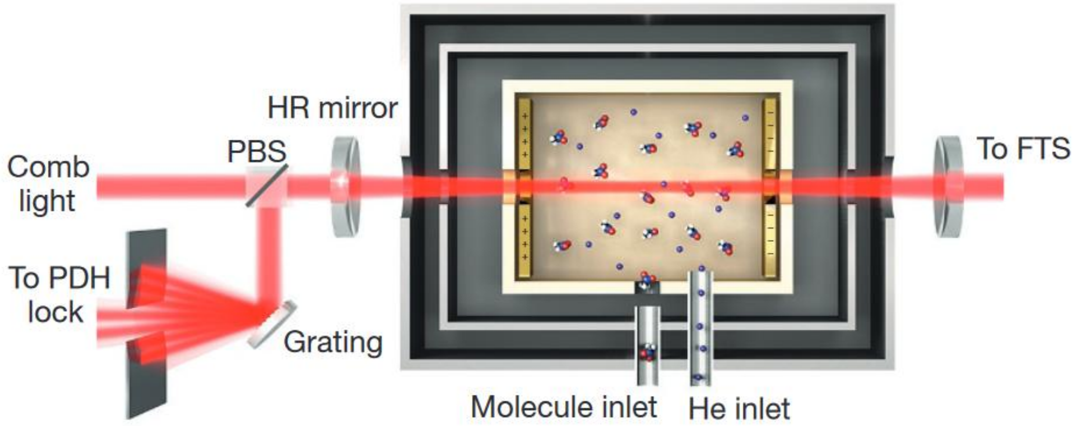

Precision ro-vibrational spectroscopy of Buffer-Gas-Cooled Molecules

- ✓ Any molecular species at rotational and translational temperatures of a few K
- ✓ Improves state selectivity → reduced spectral congestion, increased absorption cross-sections
- ✓ Restricts the distribution of velocities in the sample → narrower lineshapes
- ✓ Suppresses collisional broadening effects (when using specimens in form of beams)

Great potential for accurate line-center frequency measurements

Transferring metrological-grade spectroscopic methods to apparatuses involving cryostats

Infrared cavity-enhanced direct frequency comb spectroscopy (CE-DFCS) of large species or complex chemical mixtures: vinyl bromide, diamantane, nitromethane, naphthalene, hexamethylenetetramine,...

Spaun et al., Nature 533, 517 (2016)
Changala et al., Science 363, 49 (2019)

Quantum state-resolved ro-vibrational transitions in C60 fullerene

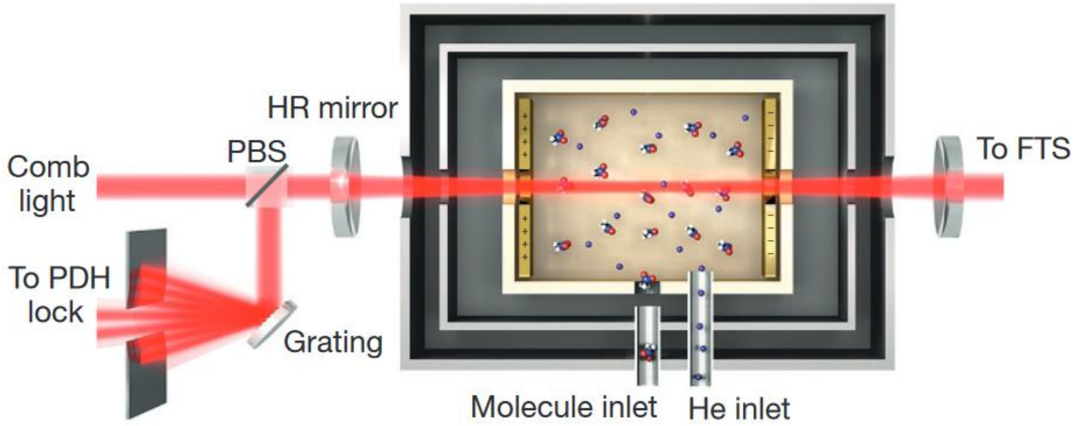

BGC Setup for Cavity-Enhanced Spectroscopy

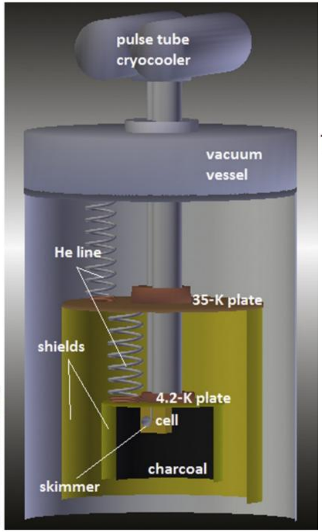

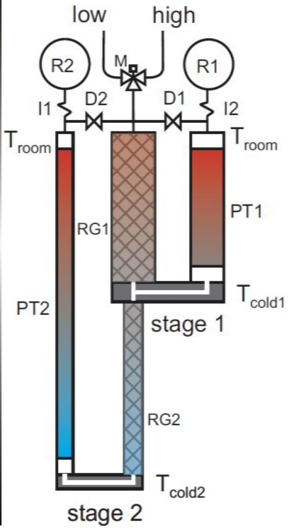

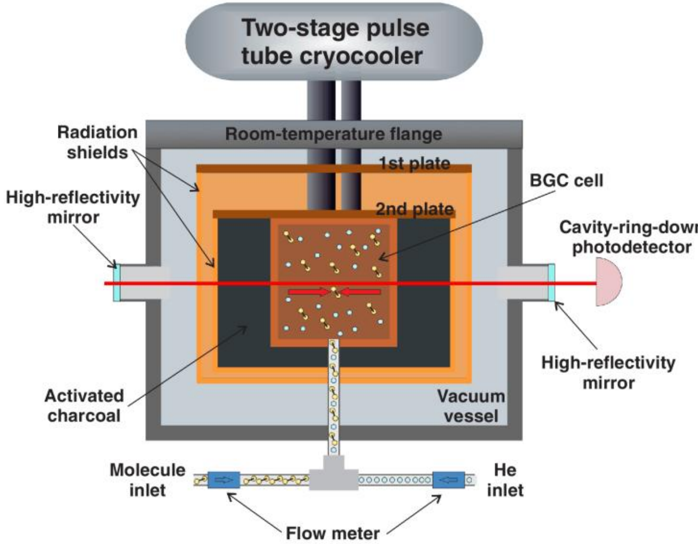

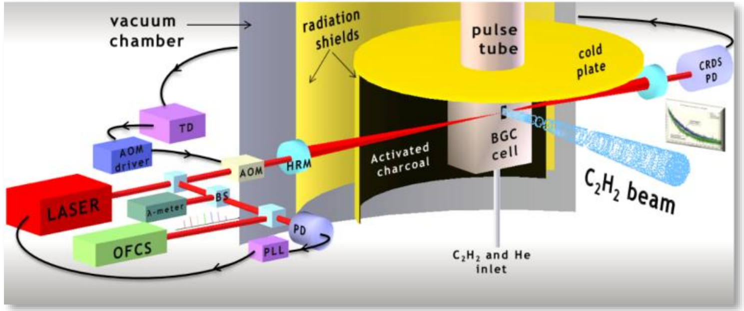

L. Santamaria et al., Astrophys. J. 801, 50 (2015)

L. Santamaria et al., PCCP 18, 16715 (2016)

BGC Setup for Cavity-Enhanced Spectroscopy

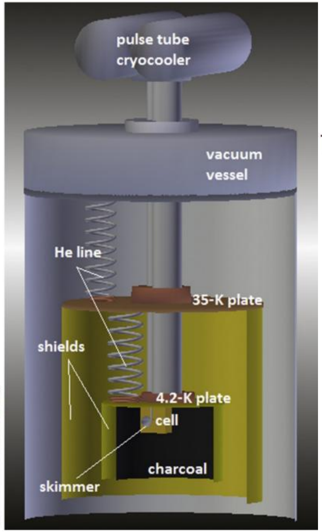

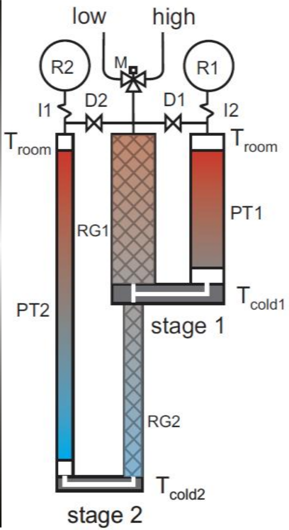

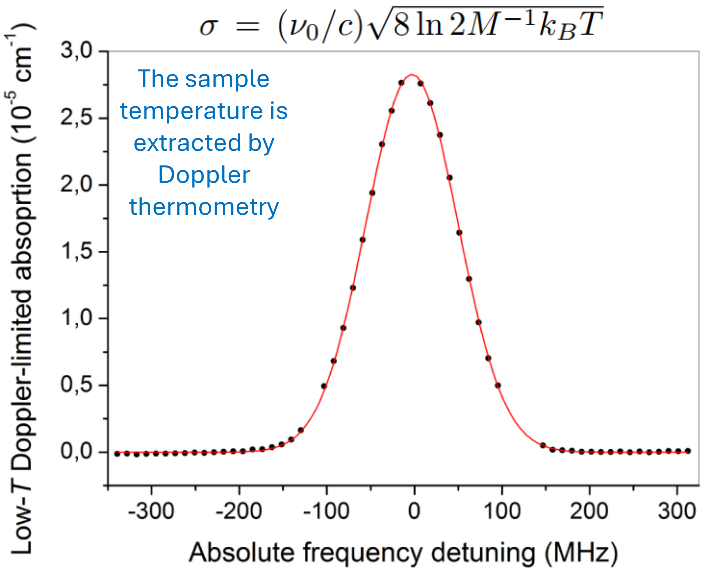

BGC Setup for Cavity-Enhanced Spectroscopy

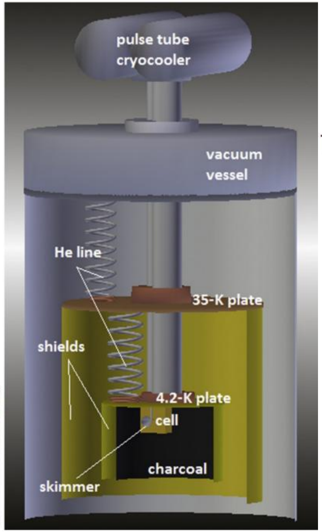

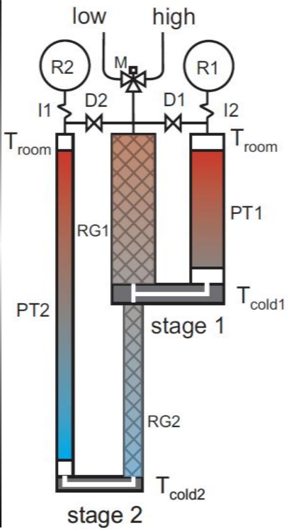

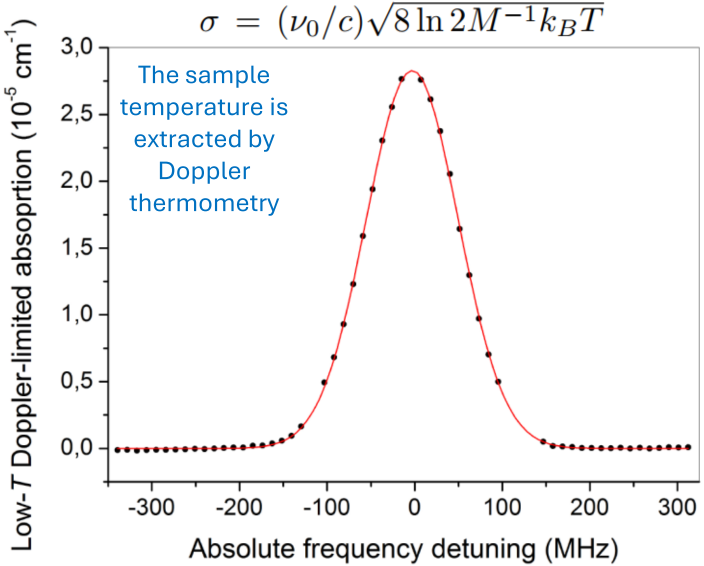

Minimize vibrations from the cryocooler on the high-finesse cavity mirrors: mechanical noise is dominated by the low-frequency components driven by the compression cycle

1. **Effective homemade mounts to** mechanically isolate the HR mirrors from the cryostat dewar by **edge-welded bellows** forming the vacuum connection

2. The mirror mounts are incorporated in **massive bars** (each resting on its own optical bench), connected by two rods girdling the cryostat dewar

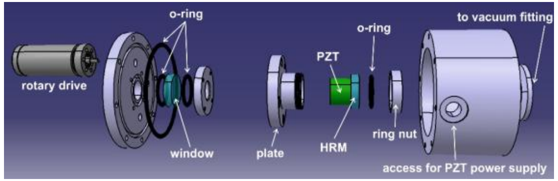

3. Additional **Vulcuren damping elements** are placed in the points of the apparatus most stressed by vibrations

V. Di Sarno et al., Optica 6, 436 (2019)

Lamb-dip Saturated-absorption Cavity Ring-down (SCAR)

Deviations from a pure exponential in the intra-cavity power due to sample saturation are exploited to retrieve in each decay both the linear and the saturated molecular absorption → get rid of spurious background fluctuations which prevent from achieving the ultimate detection limit in CRDS → **enhanced detection sensitivity**

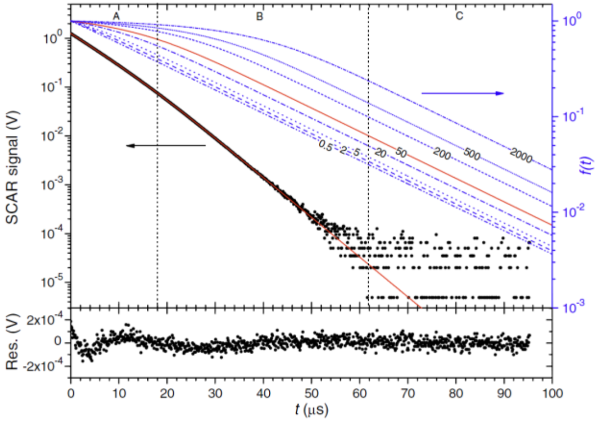

G. Giusfredi et al., Phys. Rev. Lett. 104, 110801 (2014)

$$I_{\mathrm{cav}}(t) = I_{\mathrm{cav},0}\, e^{-\gamma_c t} f(t)$$

$$S(t) = I_{\mathrm{cav}}(t)\,/I_{\mathrm{sat}}$$

$$I_{\mathrm{sat}} = \frac{4\pi^2 \hbar\, c\, \Gamma^2}{3\lambda^3 A}$$

During the first part of the decay, empty-cavity losses are measured (the high saturation level of the gas makes it *practically transparent* to radiation); as the intra-cavity radiation intensity and hence the saturation parameter *S*(*t*) decreases, the gas becomes absorbing again and the decay time returns to the unsaturated ring-down time (linear absorption).

Line-profile fitting routine expressly developed for Lamb dips

(inhomogeneous broadening regime)

$$\mathcal{V}(t) = \mathcal{A} + \mathcal{B}\, e^{-\gamma_c t}\, f(t;\gamma_c,\gamma_g,U_g(\nu))$$

$$\dot{f} = -\frac{2\,\gamma_g}{1+\sqrt{1+e^{-\gamma_c t} f(t)\, U_g(\nu)}} f(t)$$

γ_c **empty-cavity decay rate**

γ_g **linear absorption**

$U_g(\nu)$ **dip saturation profile**

VS

$$\alpha_{\mathrm{CRD}} = \frac{1}{c}\left[\frac{1}{\tau(\nu)} - \frac{1}{\tau_0}\right]$$

Conventional CRDS

R. Aiello et al., Photonics Research 10, 1803 (2022)

Lamb-dip SCAR: room-*T* pilot experiment

C_2H_2 ($\nu_1+\nu_3+\nu_4 \leftarrow \nu_4$) R(14)e line at 1523.92 nm (6562 cm^{-1})

24-bit oscilloscope

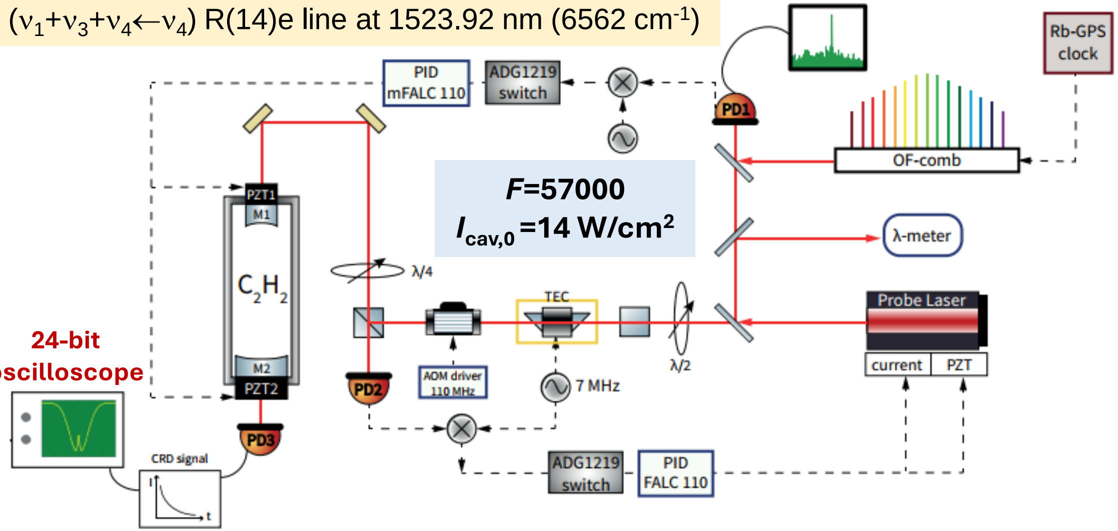

***F*=57000**
***I*$_{cav,0}$=14 W/cm^2**

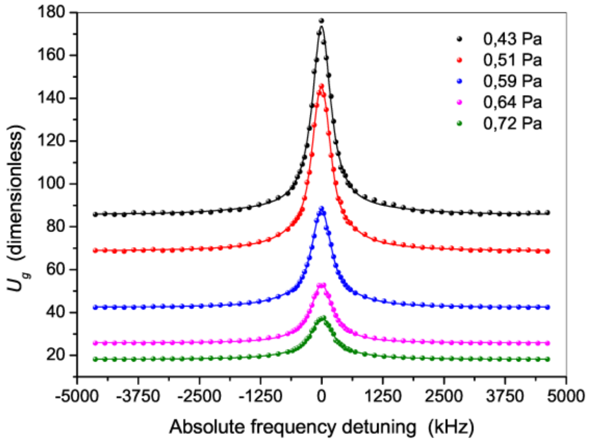

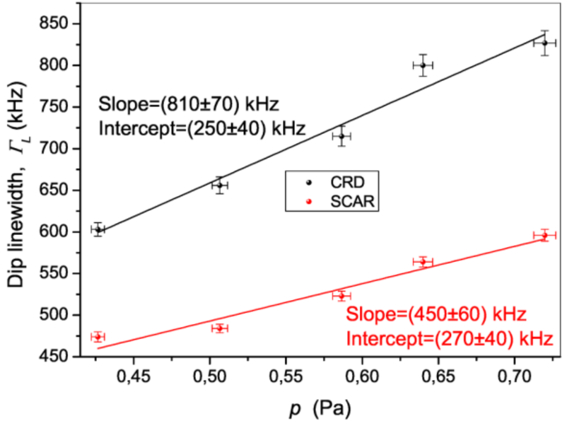

- ✓ Saturation broadening effects are left out of the widths in the U_g dip profiles ⇒ Lamb-dip FWHMs (Lorentzian fit) are reduced by 40%
- ✓ SNR increases by 90%, up to 110
- ❑ **The intercept (270 kHz) is consistent with the transit-time broadening contribution (at room *T*)**

PDH-locked Crossed-pol SCAR

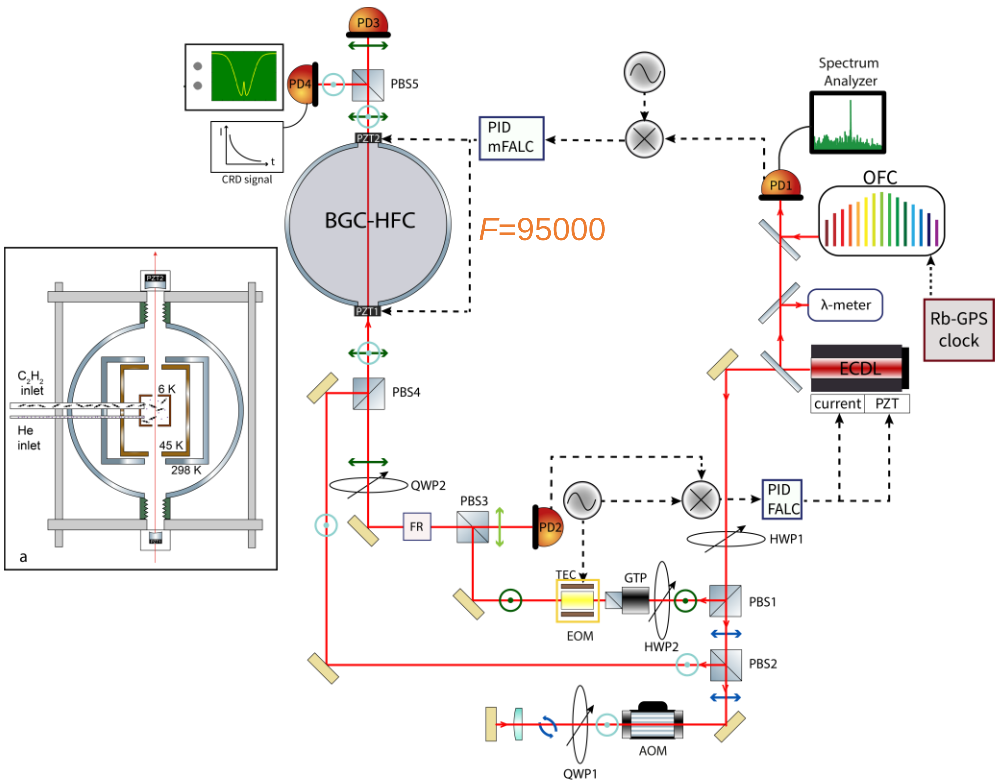

- Two orthogonally polarized laser beams are used, one for PDH-locking and the other for SCAR spectroscopy of the BGC sample → fast acquisition of ring-down events (800 Hz) without interrupting PDH locking

- The BGC-HFC length is controlled by phase-locking the beat note between the ECDL and the OFCS to a local oscillator, via two PZTs

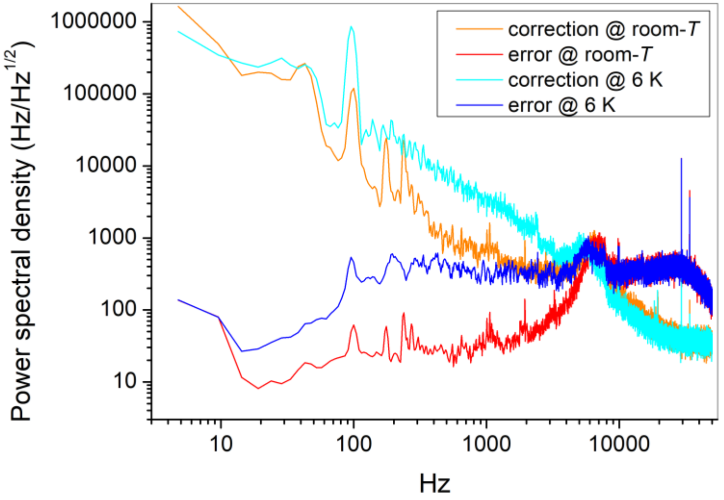

The overall lock chain is characterized by the FFT of the mFALC circuit error and correction signals

✓ A locking bandwidth around 9 kHz is achieved

Absolute determination of spectroscopic parameters

The SCAR beam frequency is tuned across the target transition

C_2H_2 ($\nu_1+\nu_3$) R(1)e line at 6561 cm^{-1}

Each dip profile is fitted with a Lorentzian lineshape to extract the line-center frequency and the FWHM

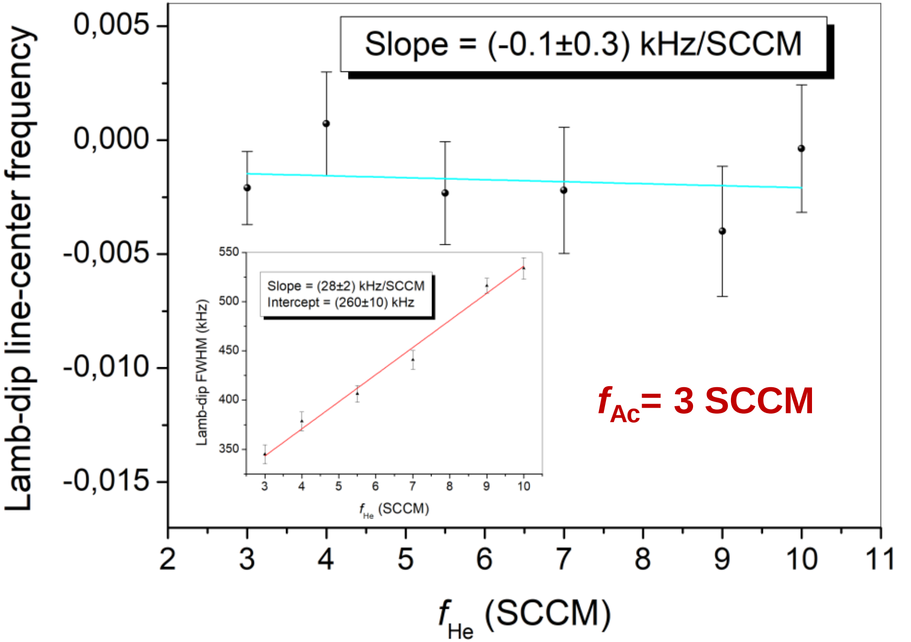

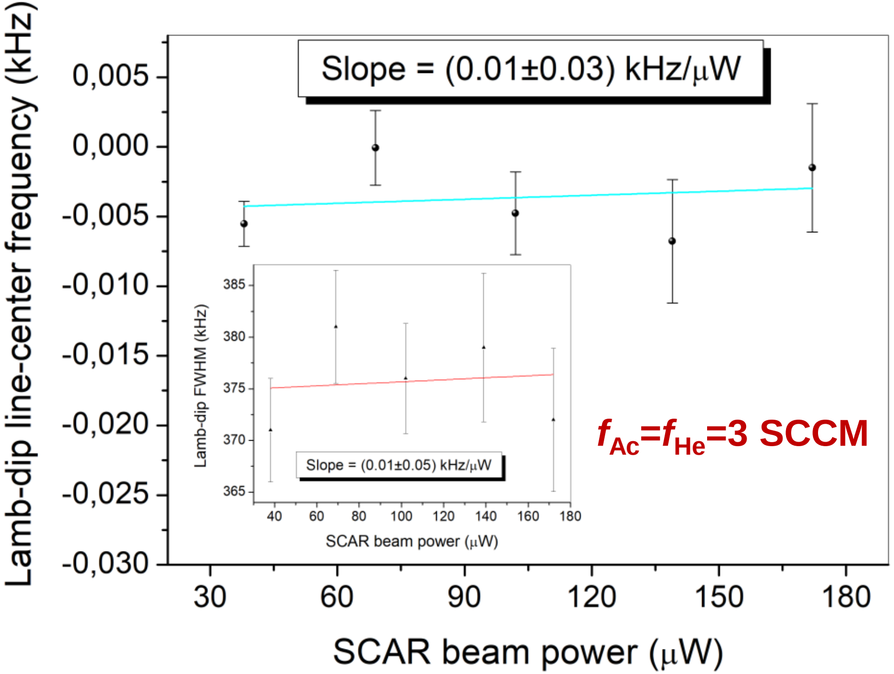

- foreign collisional-broadening coefficient: (28±2) kHz/SCCM
- self collisional-broadening coefficient: (30±5) kHz/SCCM
- SCAR analysis excludes saturation broadening effects
- Collisional/power shift coefficients are not significantly estimated

10^{-12}-level Frequency Metrology of Cold Ro-vibrational Spectra

nature communications

Article

https://doi.org/10.1038/s41467-022-34758-9

Absolute frequency metrology of buffer-gas-cooled molecular spectra at 1 kHz accuracy level

BGC + Lamb-dip + SCAR

Received: 28 July 2022

Accepted: 3 November 2022

Published online: 16 November 2022

Roberto Aiello[1], Valentina Di Sarno[1], Maria Giulia Delli Santi[1], Maurizio De Rosa[1,2], Iolanda Ricciardi[1,2], Paolo De Natale[3], Luigi Santamaria[4], Giovanni Giusfredi[5] & Pasquale Maddaloni[1,2]

ν_0 = (196 696 652 914.3 ± 1.2) kHz

Contribution	Uncertainty (kHz)
Statistical	1.1
Foreign collisional shift	0.01
Self collisional shift	0.01
Power shift	0.2
GPS-based reference chain	0.5
Second-order Doppler shift	0.02
Lamb-dip profile fit	0.07
Total	**1.2 ($6 \cdot 10^{-12}$)**

→ National optical fiber link

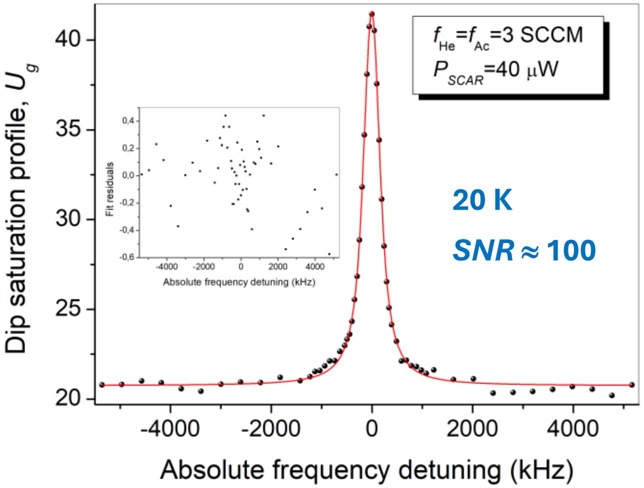

20 K

***SNR* ≈ 100**

FWHM = (340±10) kHz =

collisional broadening: (170±30) kHz
→ beam instead of cell specimen

+ transit time: (70±5) kHz
→ two-photon Ramsey fringes

+ residual laser emission linewidth
→ improve spectral properties of the probe laser

Time Stability of the Proton-to-Electron Mass Ratio

	Transition	Energy scaling
Atomic	Gross structure	Ry
	Fine structure	$\alpha^2 Ry$
	Hyperfine structure	$\alpha^2(\mu/\mu_B)Ry$
Molecular	Electronic structure	Ry
	Vibrational structure	$\beta^{-1/2}Ry$
	Rotational structure	$\beta^{-1}Ry$

$$\frac{1}{\frac{\nu(M)}{\nu(Cs)}}\frac{\partial\left[\frac{\nu(M)}{\nu(Cs)}\right]}{\partial t} = -\frac{1}{2\beta}\frac{\partial\beta}{\partial t} - 2.83\frac{1}{\alpha}\frac{\partial\alpha}{\partial t} - \frac{1}{\frac{\mu_{Cs}}{\mu_B}}\frac{\partial\left(\frac{\mu_{Cs}}{\mu_B}\right)}{\partial t}$$

where limits on α and μ_{Cs}/μ_B are inferred from atomic-clock measurements

R.M. Godun et al., PRL 113, 210801 (2014)

Measure the frequency of a ro-vibrational molecular transition relative to the Cs clock hyperfine transition

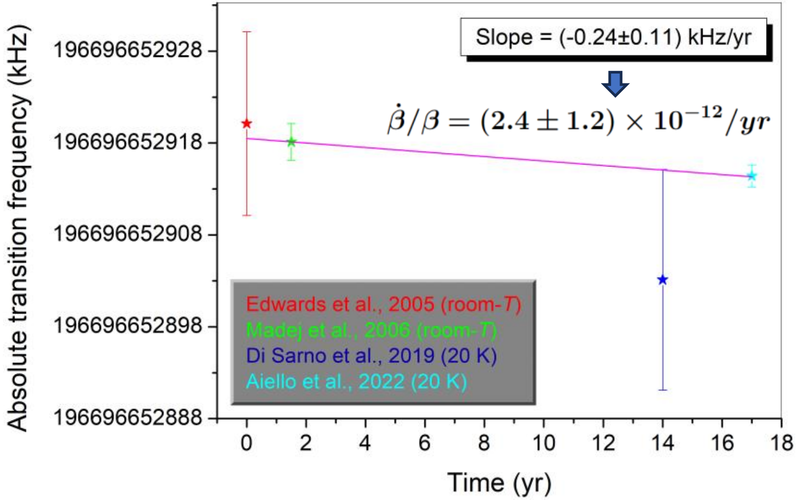

Time Stability of the Proton-to-Electron Mass Ratio

	Transition	Energy scaling
Atomic	Gross structure	Ry
	Fine structure	$\alpha^2 Ry$
	Hyperfine structure	$\alpha^2(\mu/\mu_B)Ry$
Molecular	Electronic structure	Ry
	Vibrational structure	$\beta^{-1/2}Ry$
	Rotational structure	$\beta^{-1}Ry$

$$\frac{1}{\frac{\nu(M)}{\nu(Cs)}}\frac{\partial\left[\frac{\nu(M)}{\nu(Cs)}\right]}{\partial t} = -\frac{1}{2\beta}\frac{\partial\beta}{\partial t} - 2.83\frac{1}{\alpha}\frac{\partial\alpha}{\partial t} - \frac{1}{\frac{\mu_{Cs}}{\mu_B}}\frac{\partial\left(\frac{\mu_{Cs}}{\mu_B}\right)}{\partial t}$$

where limits on α and μ_{Cs}/μ_B are inferred from atomic-clock measurements

R.M. Godun et al., PRL 113, 210801 (2014)

Measure the frequency of a ro-vibrational molecular transition relative to the Cs clock hyperfine transition

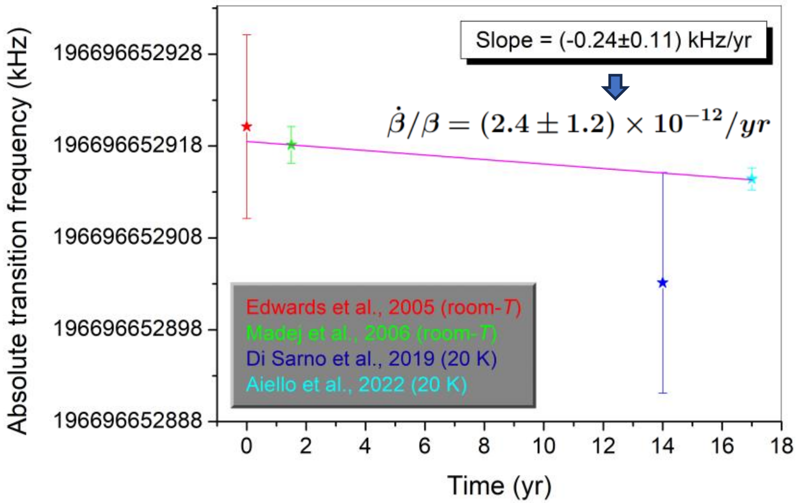

$$\dot\beta/\beta = (0.30 \pm 1.0) \times 10^{-14}/\mathrm{yr}$$

Ultracold atoms in a dual-species MOT are photoassociated into a weakly bound state; the molecules are transferred to the target internal state by STIRAP and irradiated with a microwave pulse. State selective detection of the K-Rb dimers is achieved by ionization with a pulsed laser.

J. Kobayashi et al. Nature Comm. 10, 3771 (2019)

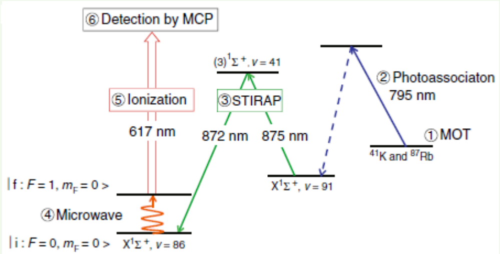

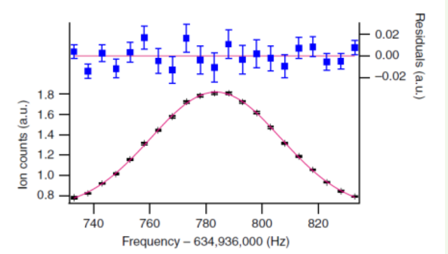

Time Stability of the Proton-to-Electron Mass Ratio

	Transition	Energy scaling
Atomic	Gross structure	Ry
	Fine structure	$\alpha^2 Ry$
	Hyperfine structure	$\alpha^2(\mu/\mu_B)Ry$
Molecular	Electronic structure	Ry
	Vibrational structure	$\beta^{-1/2}Ry$
	Rotational structure	$\beta^{-1}Ry$

$$\frac{1}{\frac{\nu(M)}{\nu(Cs)}}\frac{\partial\left[\frac{\nu(M)}{\nu(Cs)}\right]}{\partial t} = -\frac{1}{2\beta}\frac{\partial\beta}{\partial t} - 2.83\frac{1}{\alpha}\frac{\partial\alpha}{\partial t} - \frac{1}{\frac{\mu_{Cs}}{\mu_B}}\frac{\partial\left(\frac{\mu_{Cs}}{\mu_B}\right)}{\partial t}$$

where limits on α and μ_{Cs}/μ_B are inferred from atomic-clock measurements

R.M. Godun et al., PRL 113, 210801 (2014)

Measure the frequency of a ro-vibrational molecular transition relative to the Cs clock hyperfine transition

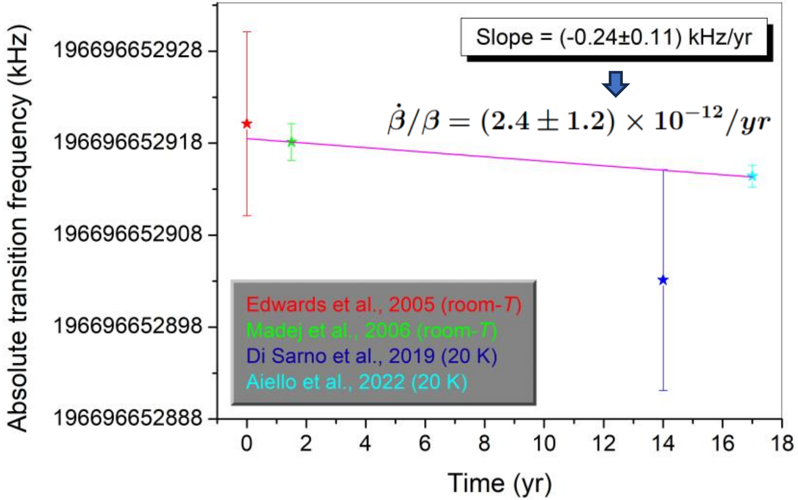

Supremo INFN-Csn2

- Constrain over a-few-year timescale the temporal variation of $\beta = m_p/m_e$ at a level of 10^{-15}/yr $\Rightarrow$ test of string-type theories seeking to unify the four known fundamental interactions

C.J.A.P. Martins, Rep. Prog. Phys. 80, 126902 (2017)

$$\dot{\beta}/\beta = (0.30 \pm 1.0) \times 10^{-14}/\text{yr}$$

Ultracold atoms in a dual-species MOT are photoassociated into a weakly bound state; the molecules are transferred to the target internal state by STIRAP and irradiated with a microwave pulse. State selective detection of the K-Rb dimers is achieved by ionization with a pulsed laser.

J. Kobayashi et al. Nature Comm. 10, 3771 (2019)

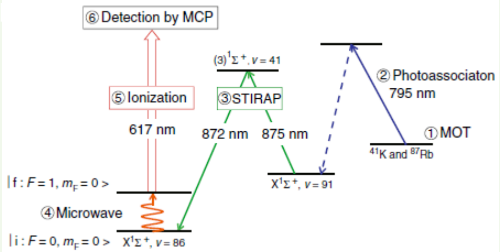

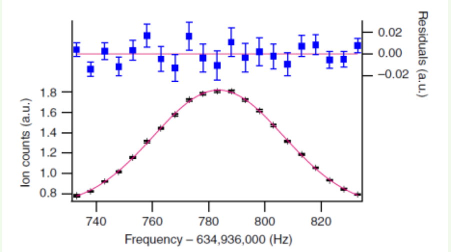

Time stability of β: future perspectives

Exciting 2-photon Ramsey fringes on the BGC beam

A. Shelkovnikov et al., Phys. Rev. Lett. 100, 150801 (2008)

acetylene passes the baton...

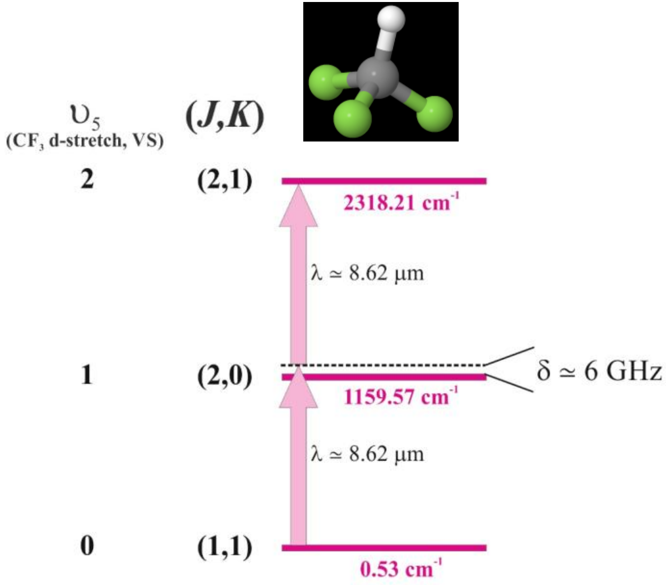


4948 Vol. 45, No. 17 / 1 September 2020 / Optics Letters Letter

Optics Letters

Absolute frequency stabilization of a QCL at 8.6 μm by modulation transfer spectroscopy

Edoardo Vicentini,[1,2,*] Alessio Gambetta,[1,2] Nicola Coluccelli,[1,2] Valentina Di Sarno,[3,4] Pasquale Maddaloni,[3,4] Paolo De Natale,[3] Antonio Castrillo,[5] Livio Gianfrani,[5,4] Paolo Laporta,[1,2] and Gianluca Galzerano[1,2]

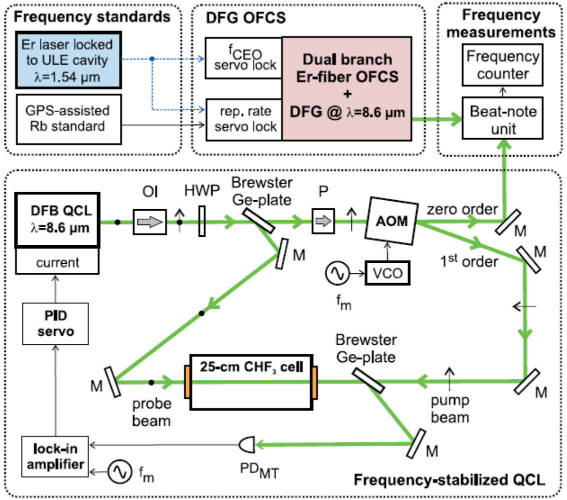

$^rR_{44}(62)$ ro-vibrational line (ν_5 vibrational band)

MTS is used to achieve frequency stabilization of an 8.6-μm QCL against a CHF_3 Lamb-dip absorption → stability and accuracy: $4\cdot10^{-12}$ (at 100 s) and $3\cdot10^{-10}$, as characterized via an OFCS stabilized against an Er-fiber laser locked to a high-finesse ULE optical cavity

Time stability of β: future perspectives

Exciting 2-photon Ramsey fringes on the BGC beam

A. Shelkovnikov et al., Phys. Rev. Lett. 100, 150801 (2008)

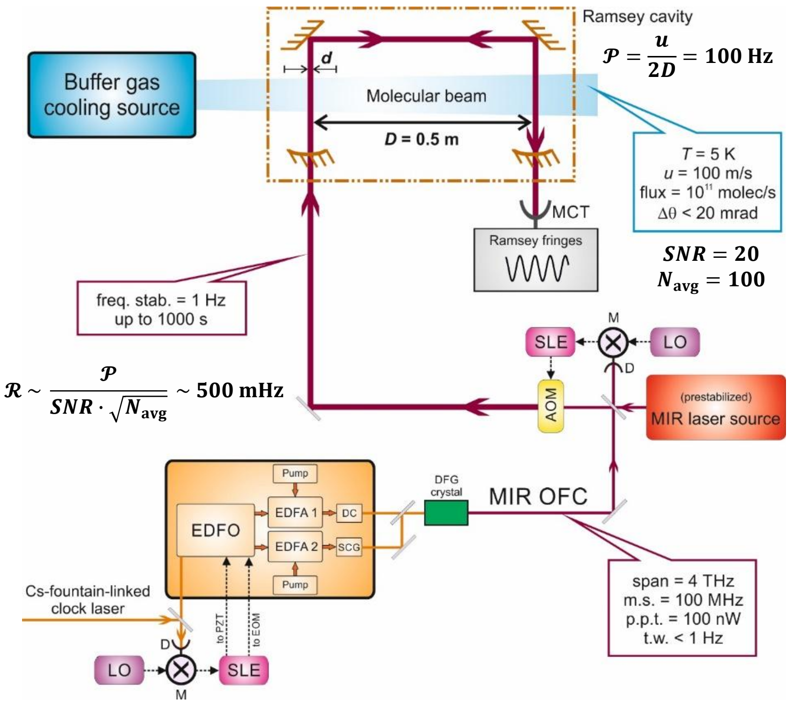

$$\mathcal{R}_{\text{frac}} \sim 5 \times 10^{-15}$$

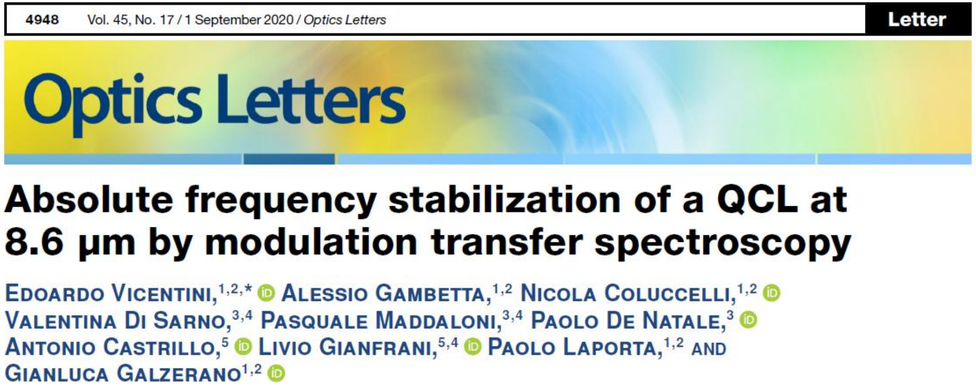

4948 Vol. 45, No. 17 / 1 September 2020 / Optics Letters **Letter**

Optics Letters

Absolute frequency stabilization of a QCL at 8.6 μm by modulation transfer spectroscopy

EDOARDO VICENTINI,[1,2,*] ALESSIO GAMBETTA,[1,2] NICOLA COLUCCELLI,[1,2] VALENTINA DI SARNO,[3,4] PASQUALE MADDALONI,[3,4] PAOLO DE NATALE,[3] ANTONIO CASTRILLO,[5] LIVIO GIANFRANI,[5,4] PAOLO LAPORTA,[1,2] AND GIANLUCA GALZERANO[1,2]

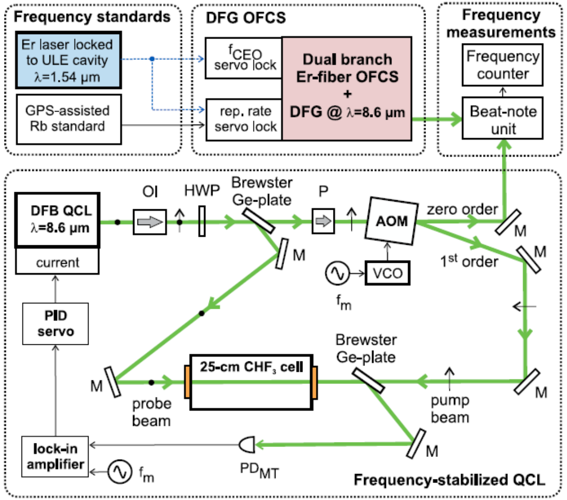

$^rR_{44}(62)$ ro-vibrational line (ν_5 vibrational band)

MTS is used to achieve frequency stabilization of an 8.6-μm QCL against a CHF_3 Lamb-dip absorption → stability and accuracy: $4 \cdot 10^{-12}$ (at 100 s) and $3 \cdot 10^{-10}$, as characterized via an OFCS stabilized against an Er-fiber laser locked to a high-finesse ULE optical cavity

Italian Quantum Backbone

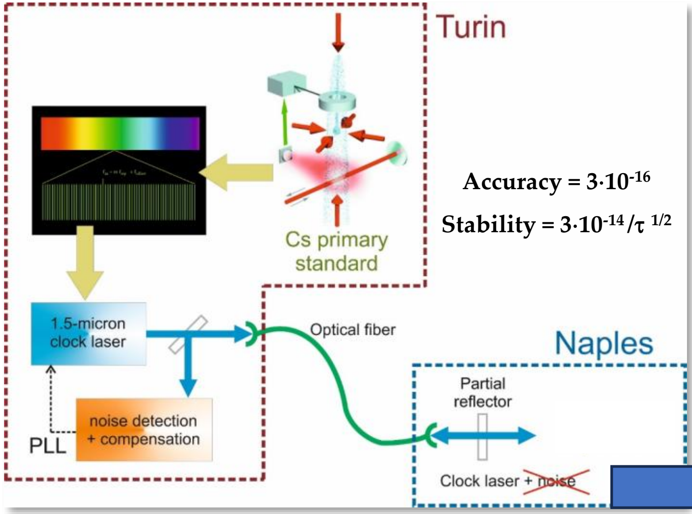

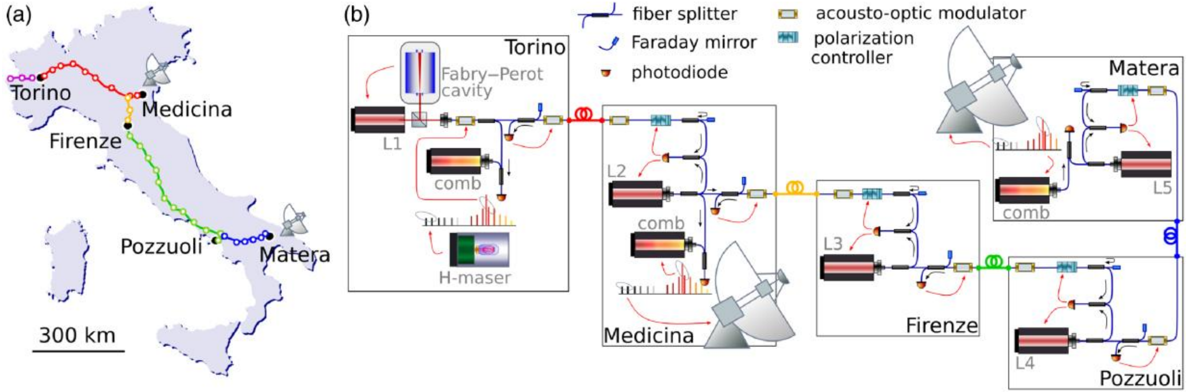

the clock laser stabilizes our local OFC

KEY SPECIFICATIONS

- Comb Spacing 250 MHz
- Accuracy 10^{-17} (τ >100 s)
- Stability: 1×10^{-16} in 1 s, 1×10^{-18} in 1000 s
- Operational Range from 500 nm to 2 µm
- Integrated Phase Noise <100 mrad [100 Hz-2 MHz]

A 1.5-micron laser (clock laser), continuosly referenced to the primary Cs fountain (or Yb lattice clock) via an OFC, is disseminated through a 800-km-long optical fiber. Part of the laser radiation is reflected back and used to cancel the phase noise accumulated during the fiber propagation

Spectroscopic probe laser

Research Article Vol. 7, No. 8 / August 2020 / *Optica* 1031

optica

Common-clock very long baseline interferometry using a coherent optical fiber link

Cecilia Clivati,[1,*] Roberto Aiello,[2,3] Giuseppe Bianco,[4] Claudio Bortolotti,[5] Paolo De Natale,[2] Valentina Di Sarno,[2,3] Pasquale Maddaloni,[2,3] Giuseppe Maccaferri,[5] Alberto Mura,[1] Monia Negusini,[5] Filippo Levi,[1] Federico Perini,[5] Roberto Ricci,[1,5] Mauro Roma,[5] Luigi Santamaria Amato,[4,6] Mario Siciliani de Cumis,[4,6] Matteo Stagni,[5] Alberto Tuozzi,[6] and Davide Calonico[1]

Fifth-force Searches

Set new bounds on putative long-range (Angstrom scale) hadron-hadron interactions (as postulated by Supersymmetry) below $10^{-10}\alpha$

E.J. Salumbides et al., New J. Phys. 17, 033015 (2015)

Denoting by $N_{1,2}$ the nucleon numbers for each atom in the molecule, the occurrence of spin-independent fifth forces with coupling strength β can be phenomenologically parameterized by a Yukawa-type potential with an effective range λ

$$V_5(r) = \hbar c \frac{\beta}{\alpha} N_1 N_2 \frac{\exp\{-r/\lambda\}}{r} \equiv \hbar c \frac{\beta}{\alpha} N_1 N_2 Y(r,\lambda)$$

By treating the extra potential as a perturbation, and considering the rovibrational transition (v', J') ← (v'', J''), the contribution of a fifth force on the rovibrational transition energy is

$$\frac{\langle \Delta V_{5,\lambda} \rangle}{\hbar c} = \frac{N_1 N_2 \beta}{\alpha} \left[\langle \Psi_{v',J'}(r) | Y(r,\lambda) | \Psi_{v',J'}(r) \rangle - \langle \Psi_{v'',J''}(r) | Y(r,\lambda) | \Psi_{v'',J''}(r) \rangle \right]$$

$$\equiv \frac{N_1 N_2 \beta}{\alpha} \Delta Y_\lambda$$

$\Rightarrow$ **tiny shifts in transition frequencies**

The wavefunctions are in principle solutions of the complete Standard Model Hamiltonian (including all interactions known to date)

$$\delta E = \sqrt{\delta E_{exp}^2 + \delta E_{calc}^2}$$

$$\frac{\beta}{\alpha} < \frac{\delta E}{N_1 N_2 \hbar c \Delta Y_\lambda}$$

Any difference between the experimental value and the numerical calculation (with λ taken as a parameter) for the considered transition energy can be used to set an upper limit

Fifth-force Searches: molecular hydrogen

- The calculations for the hydrogen molecule have never been as accurate as for the hydrogen atom due to the lack of an analytic solution of the Schrödinger equation
- There is no formulation of QED theory based on a multi-electron Dirac equation

THE JOURNAL OF CHEMICAL PHYSICS **144**, 164306 (2016)

Schrödinger equation solved for the hydrogen molecule with unprecedented accuracy

Krzysztof Pachucki[1,a)] and Jacek Komasa[2,b)]
[1]*Faculty of Physics, University of Warsaw, Pasteura 5, 02-093 Warsaw, Poland*
[2]*Faculty of Chemistry, Adam Mickiewicz University, Umultowska 89b, 61-614 Poznań, Poland*

(Received 1 February 2016; accepted 17 April 2016; published online 28 April 2016)

The hydrogen molecule can be used for determination of physical constants, including the proton charge radius, and for improved tests of the hypothetical long range force between hadrons, which require a sufficiently accurate knowledge of the molecular levels. In this work, we perform the first step toward a significant improvement in theoretical predictions of H_2 and solve the nonrelativistic Schrödinger equation to the unprecedented accuracy of 10^{-12}. We hope that it will inspire a parallel progress in the spectroscopy of the molecular hydrogen. *Published by AIP Publishing.* [http://dx.doi.org/10.1063/1.4948309]

QED tests (including proton radius and mass) with HD^+ in Paul traps

S. Patra et al., Science 369, 1238 (2020)

S. Alighanbari et al., Nature Physics 19, 1263 (2023)

M. Germann et al., Phys. Rev. Res. 3, L022028 (2021)

Effective NRQED approach based on the Schrödinger equation:

- expansion of energy levels in powers of the fine structure constant
- the expansion coefficients are expressed as expectation values of effective Hamiltonians with the nonrelativistic wavefunction

$$E = E_{\mathrm{NR}} + (\alpha^2 E_{\mathrm{REL}} + \alpha^3 E_{\mathrm{QED}} + \alpha^{n\geq 4} E_{\mathrm{HO}}) + E_{\mathrm{NUC}} + \dots$$

Leading-order relativistic corrections: *mass-velocity, Darwin, orbit-orbit, spin-spin, recoil terms*

Leading-order QED corrections: *self-energy, vacuum polarization, radiative width, pair corrections*

Nuclear effects: *magnetic moment (HFS), charge distribution*

Fifth-force Searches: Experiment

1. Perform sub-kHz-accuracy line-center frequency determinations for selected HD ro-vibrational transitions in the (2,0) and (1,0) band

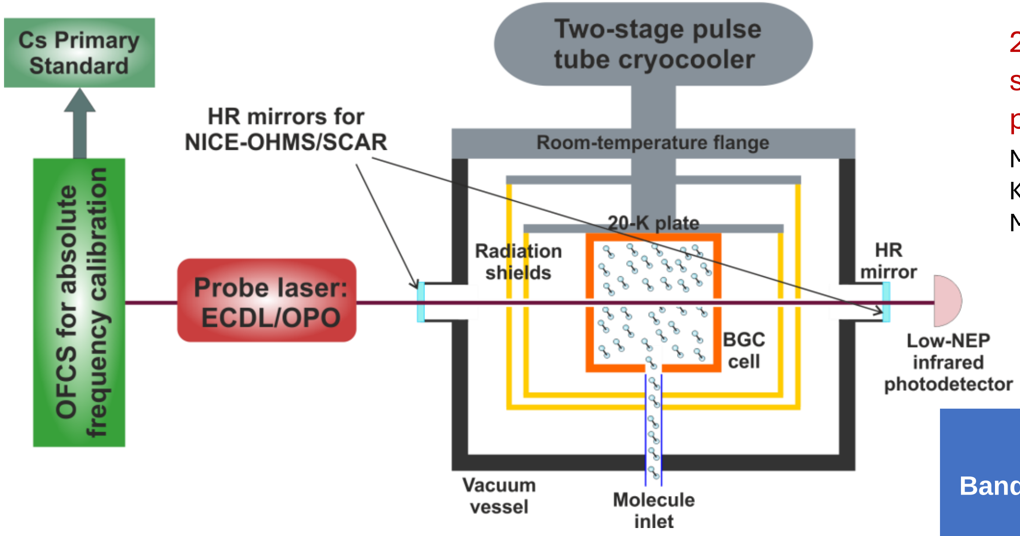

Lamb-dip SCAR Spectroscopy
on
Buffer-gas-cooled HD samples

$$\delta\nu_0 \sim \sqrt{T}\,Q(T)$$

2. Compare the experimental transition frequencies with state-of-the-art (continuously improving) ab initio theoretical predictions

M. Silkowski et al., Mol. Phys. 120, e2062471 (2022)
K. Pachucki et al., J. Chem. Phys. 144, 164306 (2016)
M. Puchalski, et al., Phys. Rev. Lett. 117, 263002 (2016)

List of selected HD ro-vibrational transitions (Hitran database)

Band	Transition	Laser wavelength (micron)	Room-*T* linestrength (cm/molec)	Einstein *A* coefficient (Hz)	Sample temperature (K)
(2,0)	R(0)	1.395	2.5E-25	1.58E-5	20
	R(1)	1.386	3.7E-25	2.15E-5	298
	R(2)	1.369	2.5E-25	2.58E-5	298
	R(3)	1.358	1.0E-25	2.95E-5	298
(1,0)	R(0)	2.690	1.0E-24	1.67E-5	20

Upgrading the spectroscopic probe laser

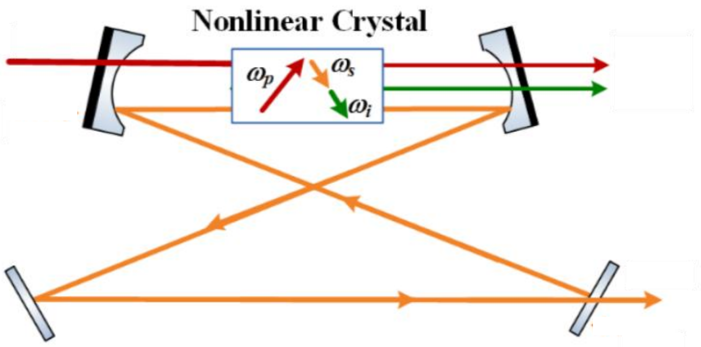

Key Features

- 1.45 - 4.0 μm (2500 - 6900 cm^{-1})
- 300 GHz (10 cm^{-1}) mode-hop-free tuning range
- Narrow linewidth: 2 MHz ($1 \cdot 10^{-5}$ cm^{-1})
- Hands-free motorized tuning
- Easy all-digital DLC pro control
- Watt class power

Both pump and signal frequencies are phase-locked to the OFCS

Upgrading the spectroscopic probe laser

	ORS
Wavelength	500–1600 nm (IBS coatings), 900–1600 nm (XTAL coatings)
Stability (MADEV at 1 s, linear drift removed)	<7 x 10^{-16} (with FS-XTAL option) <1 x 10^{-15} (with FS-IBS option) <2 x 10^{-15} (with ULE-IBS, standard system)
Linewidth	<1 Hz
Phase Noise (laser source dependent)	ULE-IBS / FS-XTAL at 10 Hz: -7 dBc/Hz / -13 dBc/Hz at 100 Hz: -47 dBc/Hz / -47 dBc/Hz at 1000 Hz: -70 dBc/Hz / -70 dBc/Hz

The Optical Reference System (ORS) delivers ultra-narrow linewidth laser light with outstanding frequency stability. The centerpiece is a high-finesse Fabry-Perot cavity (made from ULE), operated in vacuum at the point of zero thermal expansion, and actively decoupled from vibrations and acoustically isolated

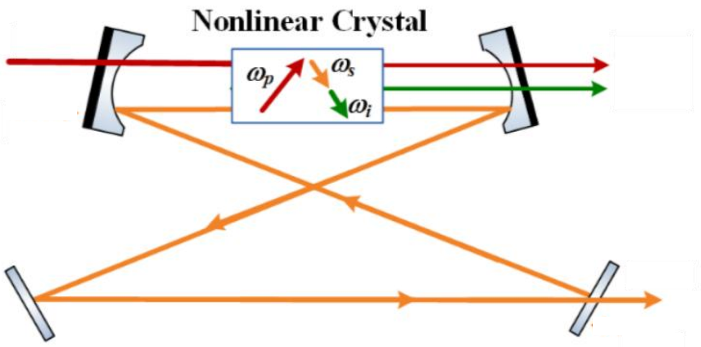

Key Features

- 1.45 - 4.0 μm (2500 - 6900 cm^{-1})
- 300 GHz (10 cm^{-1}) mode-hop-free tuning range
- Narrow linewidth: 2 MHz (1·10^{-5} cm^{-1})
- Hands-free motorized tuning
- Easy all-digital DLC pro control
- Watt class power

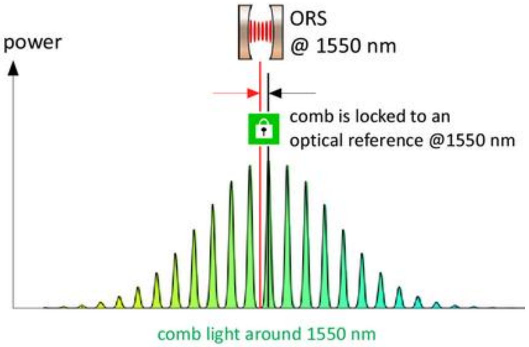

The superior spectral purity of the ORS is copied to every comb line and eventually to the OPO idler

Both pump and signal frequencies are phase-locked to the OFCS

Second-generation BGC source: ultra-low-vibration mode

Vacuum chamber with improved mechanical stability, housed on the optical bench (no longer on a perch resting on the floor)

Remote-motor bellow system
The head of the cryocooler is placed on a metal shelf, suspended by means of a system of steel tie rods, anchored to load-bearing beams in the laboratory's false ceiling

Cryomech PT415

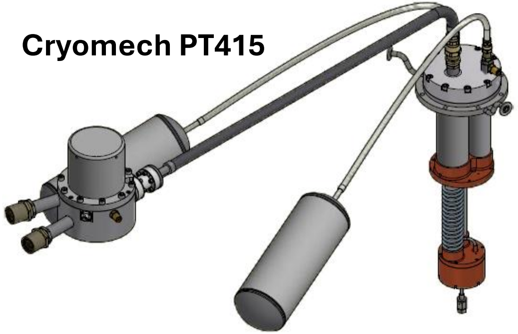

Second-generation BGC source: other upgrades

The efficiency of the collisional cooling process is maximized by introducing helium through a coil wrapped around the second buffer tube

New internal shields with optimized geometry, covered with activated charcoal (which at cryogenic temperatures acts as a vacuum pump with a speed of several thousand liters per second)

Cryogenic linear stage
Attocube ANPz102/RES/LT/HV
travel range: 5 mm
fine positioning resolution: sub-nm

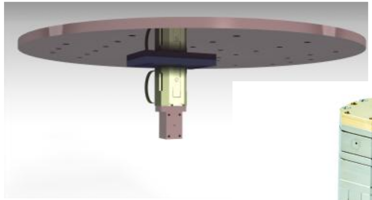

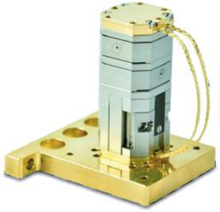

Cryogenic nano-positioner for fine alignments of the BGC molecular beam with respect to the enhancement cavity axis

C14-SCAR


C14-SCAR

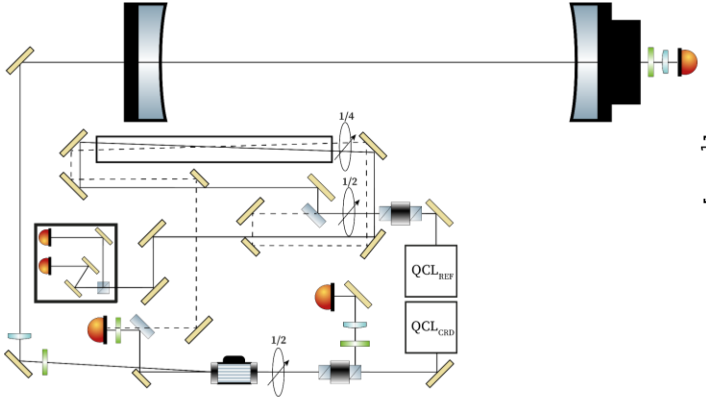
1/4
1/2
1/2
QCL$_{REF}$
QCL$_{CRD}$

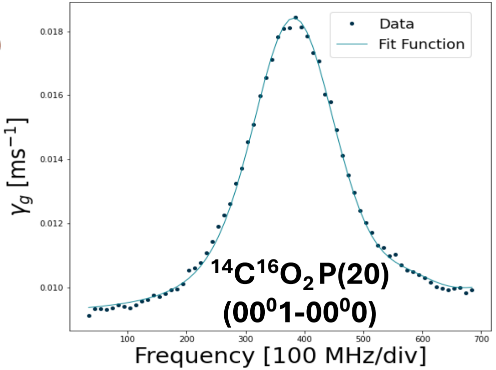
Data
Fit Function
γ_g [ms^{-1}]
Frequency [100 MHz/div]
$^{14}C^{16}O_2$ P(20)
(00^01-00^00)

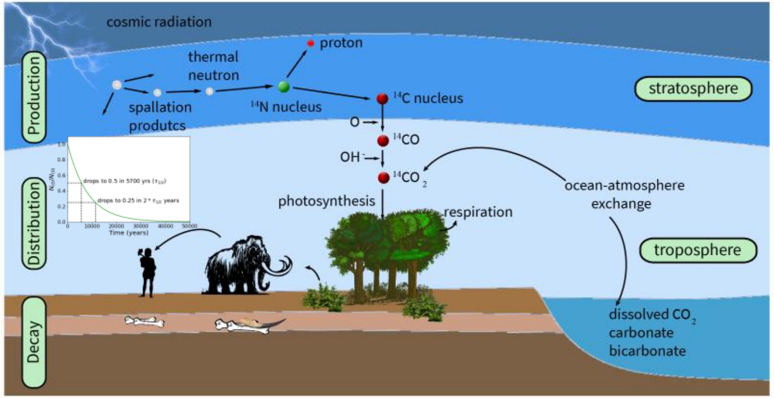
cosmic radiation
Production
Distribution
Decay
thermal neutron
proton
spallation produtcs
^{14}N nucleus
^{14}C nucleus
stratosphere
O
^{14}CO
OH
$^{14}CO_2$
photosynthesis
respiration
ocean-atmosphere exchange
troposphere
dissolved CO_2
carbonate
bicarbonate

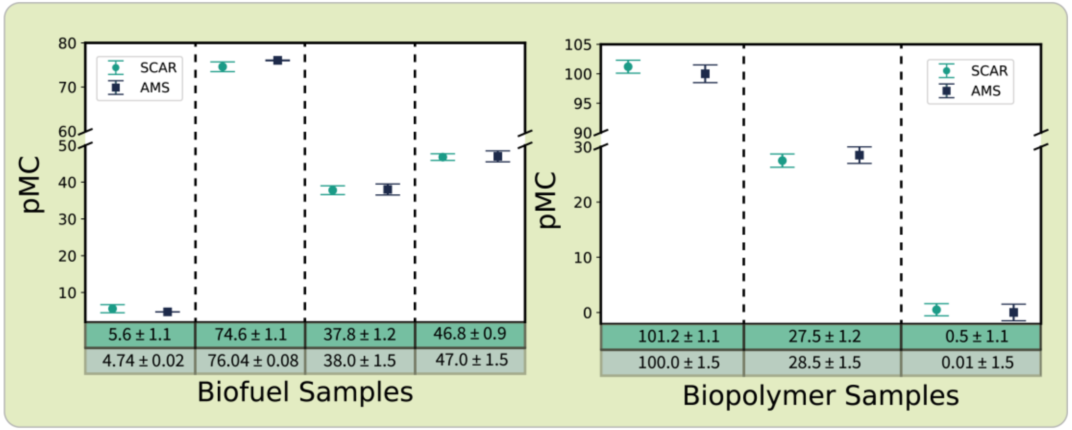
SCAR
AMS
pMC
5.6 ± 1.1
74.6 ± 1.1
37.8 ± 1.2
46.8 ± 0.9
4.74 ± 0.02
76.04 ± 0.08
38.0 ± 1.5
47.0 ± 1.5
Biofuel Samples
101.2 ± 1.1
27.5 ± 1.2
0.5 ± 1.1
100.0 ± 1.5
28.5 ± 1.5
0.01 ± 1.5
Biopolymer Samples

THz ASOPS (asynchronous optical sampling)-spectrometer

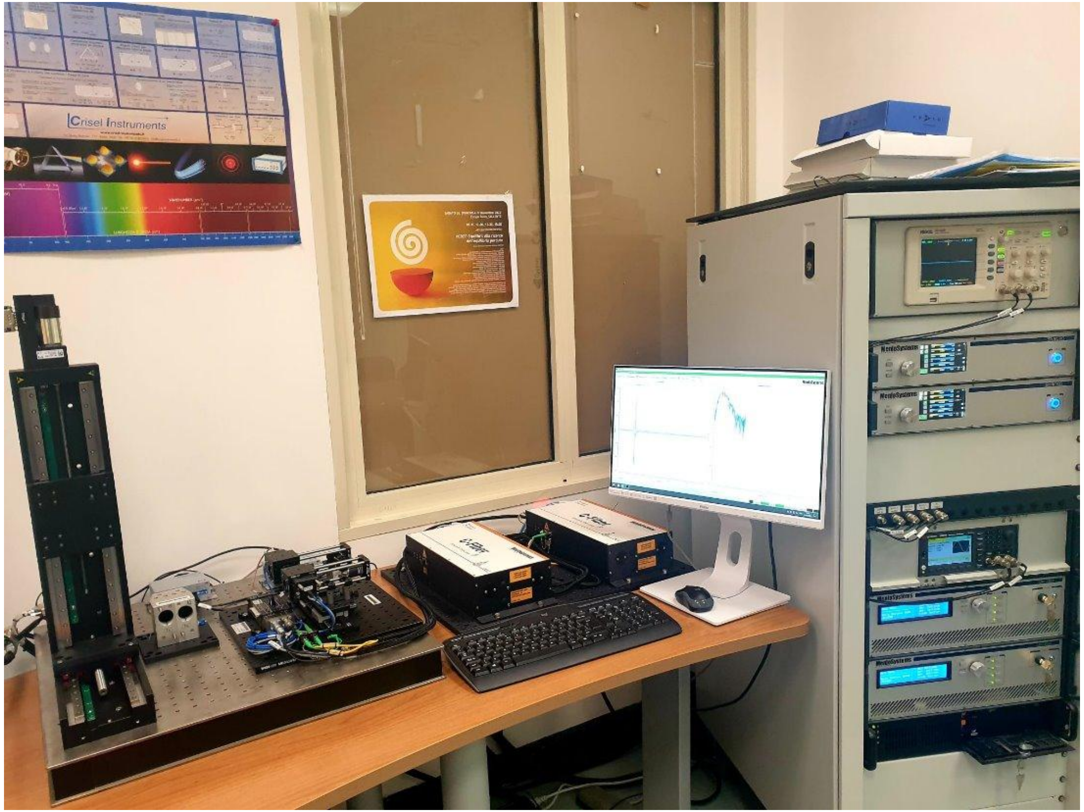

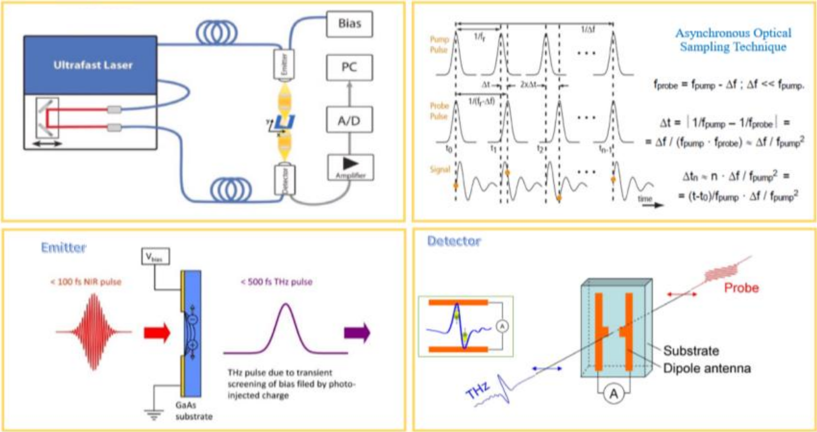

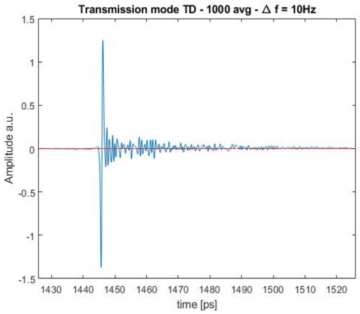

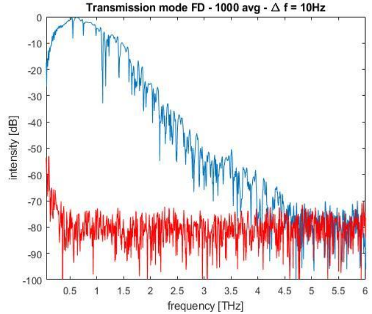

Laboratori Congiunti ASI-CNR nel settore delle Tecnologie Quantistiche
Progetto QASINO

Cold Molecules lab

Maddaloni Pasquale
Roberto Aiello
Maria Giulia Delli Santi (C-14 SCAR)
Valentina Di Sarno (THz ASOPS)
Coming soon: Luisa Boglioni, Hira Batool

Thank you !

To appreciate the beauty of a snowflake it is necessary to stand out in the cold (Aristotle)

www.ino.cnr.it